





Article

Ruthenium(II) Complexes with (3-Polyamino)phenanthrolines: Synthesis and Application in Sensing of Cu(II) Ions

Anton S. Abel^{1,2,*} , Alexei D. Averin^{1,3}, Andrey V. Cheprakov¹, Irina P. Beletskaya^{1,3,*} , Michel Meyer² 
and Alla Bessmertnykh-Lemeune^{2,4,*} 

- ¹ Department of Chemistry, Lomonosov Moscow State University, Leninskie Gory 1-3, 119991 Moscow, Russia; averin@org.chem.msu.ru (A.D.A.); avchep@avchem.ru (A.V.C.)
² Institut de Chimie Moléculaire de l'Université de Bourgogne, UMR 6302, CNRS, Université Bourgogne Franche-Comté, 9 Avenue Alain Savary, BP 47870, 21078 Dijon Cedex, France; michel.meyer@u-bourgogne.fr
³ Frumkin Institute of Physical Chemistry and Electrochemistry, Russian Academy of Sciences, Leninsky Pr. 31, 119071 Moscow, Russia
⁴ Laboratoire de Chimie, UMR 5182, CNRS, ENS de Lyon, 46 Allée d'Italie, 69364 Lyon Cedex, France
 * Correspondence: antonabel@list.ru (A.S.A.); beletska@org.chem.msu.ru (I.P.B.); alla.lemeune@ens-lyon.fr (A.B.-L.)

Abstract: This work deals with the development of water-soluble optical sensors based on ruthenium(II) tris(diimine) complexes that exhibit high molar absorptivity and are emissive in aqueous media. Palladium-catalyzed arylation of polyamines with 3-bromo-1,10-phenanthroline (Brphen) and [Ru(bpy)₂(Brphen)](PF₆)₂ (bpy = 2,2'-bipyridine) was explored to prepare Ru²⁺ complexes with 1,10-phenanthrolines (phen) substituted by linear polyamines (PAs) at position 3 of the heterocycle ([Ru(bpy)₂(phen-PA)](PF₆)₂). The most convenient synthetic pathway leading to the target molecular probes includes the preparation of phen-PA ligands, followed by ruthenium complexation using *cis*-Ru(bpy)₂Cl₂. Complexes bearing a polyamine chain directly linked to phenanthroline core are emissive in aqueous media and their quantum yields are comparable to that of parent [Ru(bpy)₃](PF₆)₂. Their structure can be easily adapted for detection of various analytes by modification of amine groups. As an example, we prepared the emissive complex **Ru(N₂P₂phen)** which is suitable for the dual channel (spectrophotometry and luminescence (ON-OFF probe)) selective detection of Cu²⁺ ions at the physiological pH levels with limits of detection (LOD) by spectrophotometry and fluorescence spectroscopy equal to 9 and 6 μM, respectively, that is lower than the action level in drinking water for copper as prescribed by the US Environmental Protection Agency.

Keywords: chemosensor; luminescence; Ru tris(diimine) complexes; 1,10-phenanthroline; cupric ions



Citation: Abel, A.S.; Averin, A.D.; Cheprakov, A.V.; Beletskaya, I.P.; Meyer, M.; Bessmertnykh-Lemeune, A. Ruthenium(II) Complexes with (3-Polyamino)phenanthrolines: Synthesis and Application in Sensing of Cu(II) Ions. *Chemosensors* **2022**, *10*, 79. <https://doi.org/10.3390/chemosensors10020079>

Academic Editor: Francesco Baldini

Received: 12 January 2022

Accepted: 11 February 2022

Published: 14 February 2022

Publisher's Note: MDPI stays neutral with regard to jurisdictional claims in published maps and institutional affiliations.



Copyright: © 2022 by the authors. Licensee MDPI, Basel, Switzerland. This article is an open access article distributed under the terms and conditions of the Creative Commons Attribution (CC BY) license (<https://creativecommons.org/licenses/by/4.0/>).

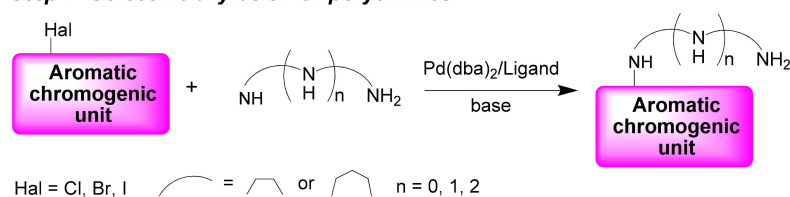
1. Introduction

The design and synthesis of abiotic molecular systems capable of signaling various guest molecules or ions by changing optical properties has spurred tremendous research efforts [1]. Being optimized, these molecular probes have many advantages, such as real-time and rapid colorimetric response, and/or beneficially exploit the high sensitivity and environmental versatility of photoluminescence spectroscopy. However, many chemosensors already reported suffer from various drawbacks such as slow response, poor chemical or photostability, irreversibility, short lifetimes, low solubility, and/or low quantum yields in aqueous media. While most analytical applications concern aqueous solutions, the optical sensing techniques in this media are still underdeveloped, because the synthesis of water-soluble receptors is generally laborious and their solubility in aqueous medium is not easily predictable. A common strategy to increase water solubility of aromatic molecules, which consists of the introduction of charged functional groups, such as carboxylates, sulfonates, or ammonium [2,3], is only of limited value for developing chemosensors, in particular for

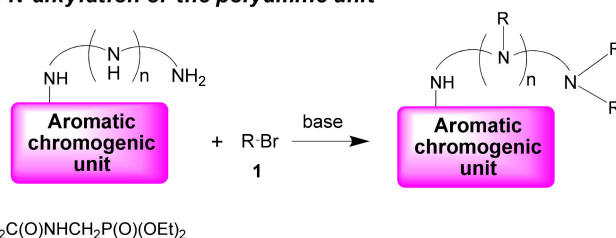
metal ions, because these donor groups can serve as alternative ligand sites for ions that strongly deteriorates selectivity.

Recently, water-soluble polyamine ionophores incorporating hydrophilic diethoxyphosphoryl-substituted amide moieties were developed by our groups (Scheme 1) [4]. The synthetic approach to these chromogenic chelators involves the selective Pd-catalyzed amination reaction (step 1) followed by their *N*-alkylation with alkyl halides bearing diethoxyphosphoryl moieties such as [(2-bromoacetyl)amino]methyl]phosphonic acid diethyl ester (1) (step 2). This strategy could be expected to be useful for a variety of chromogenic units due to the wide substrate scope of both steps involved in the reaction sequence. In this work, we report on the synthesis of chemosensors bearing mixed ligand ([Ru(bpy)₂(phen)]²⁺-type complexes as signaling groups.

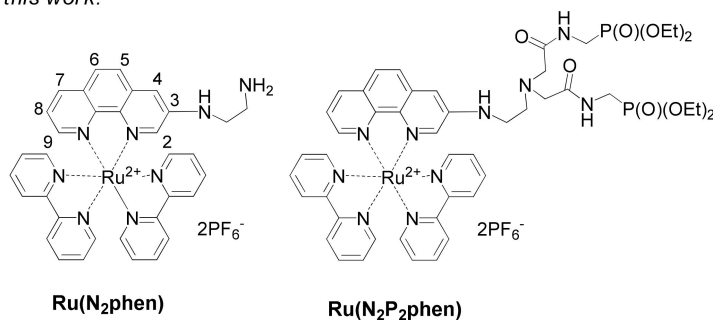
Step 1: Selective arylation of polyamines



Step 2: *N*-alkylation of the polyamine unit



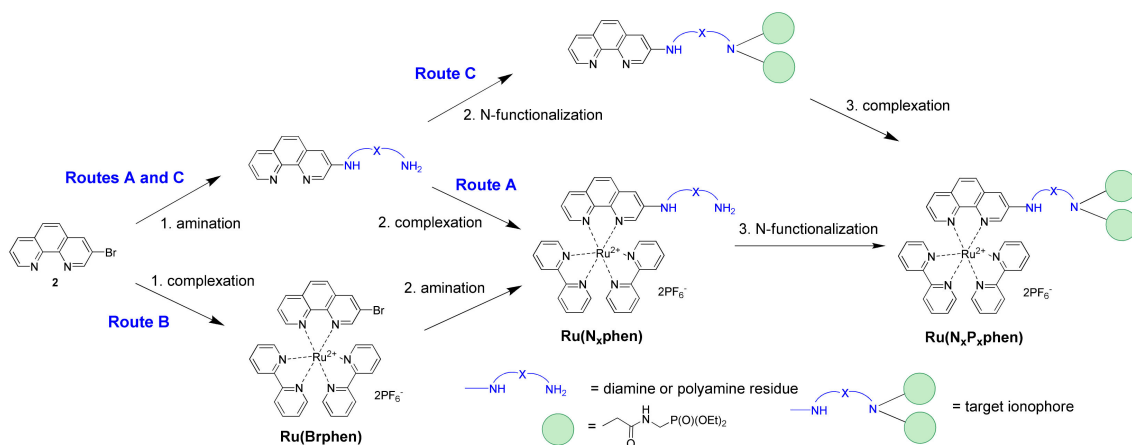
In this work:



Scheme 1. Synthetic approaches to chemosensors with polyamine ionophores and the structures of complexes investigated in this work.

The stable and biocompatible ruthenium(II) tris(diimine) complexes (diimine = bpy, phen, terpyridine) have attracted considerable attention as luminophores and been explored in labeling, sensing, and imaging of various gases (dioxygen [5], nitric oxide [6], and carbon monoxide [7]), biological analytes (DNA, sugars, methylglyoxal, thiols, and amino acids) [8–10], and anions [11–19]. In contrast to most organic dyes, these complexes can exhibit a high brightness [20] in aqueous media, in part due to the electrostatic repulsive interactions that prevent the aggregation of these charged species in aqueous media. Nevertheless, structure/sensing efficiency relationships in this series of indicators are still less well understood compared to common organic dyes, in part because these compounds are hardly accessible. For most of the reported complexes with phen ligands, the ionophore unit is located at the most reactive positions of the heterocycle, namely, 4/7 and 5/6, and attached to the signaling group by C=O, -CH=N-, or imidazole linkers.

1,10-Phenanthrolines, which bear ionophores directly connected to the aromatic scaffold, are promising ligands for development of chemosensors, as analyte uptake could be expected to exert a strong impact on both the photophysical and electrochemical properties of the corresponding ruthenium(II) complexes, thus allowing for multichannel detection of analytes. The only reported examples of such chelators are the complexes containing mixed-donor (N, O, S) macrocycles (i.e., crown-ether-type receptors fused at the central six-membered ring via positions 5 and 6 or attached at positions 4 and 7 of the heterocycle, or azacrown-type derivatives bearing two macrocycles attached at positions 4 and 7 of the phenanthroline ring) [21,22]. On the other hand, the emissive properties of ruthenium(II) tris(diimine) complexes with aminophenanthroline ligands are strongly dependent on the position of the amino-substituent attached to the heterocycle, and emission quantum yields of complexes involving 4-substituted phen ligands are expected to be low [23,24]. This could be detrimental for the sensibility of chemosensors. In contrast, the introduction of the amino substituents in the 3- or 5-position of the 1,10-phenanthroline ring results only in a small decrease in luminescence quantum yields compared to that of the parent complex $[\text{Ru}(\text{bpy})_2(\text{phen})](\text{PF}_6)_2$, while the brightness of the complexes with the 3-substituted ligands is comparable to that of the parent complex. In these Ru^{2+} complexes, the signaling and receptor units are directly connected, and HOMO is localized on the aminophenanthroline ligand [24]. As a consequence, analyte binding by the nitrogen atom of the substituent should strongly affect the HOMO energy, leading presumably to significant modulation of the absorption and emission properties. We were interested in preparing complexes bearing polyamine ionophores, which are widely used in detection and are efficient for binding both cationic and anionic analytes depending on the degree of their protonation and can be easily adapted to the analyte structure using functionalization of amino groups. Various synthetic approaches were investigated to propose a reliable approach to the preparation of these molecular probes (Scheme 2).



Scheme 2. The three tested synthetic routes for the preparation of $\text{Ru}(\text{N}_x\text{P}_x\text{phen})$.

After preparing $\text{Ru}(\text{N}_2\text{P}_2\text{phen})$ and $\text{Ru}(\text{N}_2\text{phen})$ in reasonable yield, the optical properties of these chromophores in aqueous media were investigated followed by studies of their proton sensitivity and sensing properties towards metal ions. It was demonstrated that despite a high brightness of both complexes, only $\text{Ru}(\text{N}_2\text{P}_2\text{phen})$ allows for dual channel optical detection of Cu^{2+} ions in aqueous media including tap water.

2. Materials and Methods

2.1. Reagents

Unless otherwise noted, all chemicals and starting materials were obtained commercially from Acros (via Fisher Scientific, Illkirch, France) and Aldrich–Sigma Co. (via Merck Co., Darmstadt, Germany) and used without further purification. Preparative column chro-

matography was carried out using silica gel 60 (40–63 μm) from Merck Co. (Darmstadt, Germany). Dioxane was distilled successively over NaOH and sodium under argon, CH_2Cl_2 and CH_3CN were distilled over CaH_2 , chloroform was distilled over P_2O_5 , and MeOH was used freshly distilled. [(2-Bromoacetylamino)methyl]phosphonic acid diethyl ester (**1**) was obtained according to a known procedure [25]. $\text{Pd}(\text{dba})_2$ was synthesized according to a known method [26] and used without recrystallization. 3-Bromo-1,10-phenanthroline (**2**) was synthesized according to the procedure in [27] and purified by column chromatography followed by recrystallization from boiling acetone. $N^1, N^{1'}$ -(ethane-1,2-diyl)diethane-1,2-diamine (**5e**) was prepared by treatment of tetraethylenepentamine dihydrochloride with 2.5 M solution of KOH in methanol. The starting complex, *cis*- $\text{Ru}(\text{bpy})_2\text{Cl}_2$, was synthesized from $\text{RuCl}_3 \cdot 3\text{H}_2\text{O}$ according to a known method [28].

2.2. Apparatus

The pH measurements were carried out using Mettler Toledo apparatus with a combined electrode LE438. The electrode was calibrated with commercial buffers (pH = 4.01 and 7.00). UV–Vis spectra were registered with an Agilent Cary 60 device in quartz cuvette (Hellma, $l = 1$ cm). Fluorescence spectra were obtained with a Horiba Jobin Yvon Fluoromax-2 apparatus in quartz cuvette (Hellma, $l = 1$ cm). Luminescence quantum yields were determined relative to $\text{Ru}(\text{bpy})_3(\text{PF}_6)_2$ in aerated acetonitrile according to a standard procedure [29].

^1H , ^{31}P , and ^{13}C NMR spectra were registered with a Bruker Avance-400 spectrometer in chloroform- d_1 , methanol- d_4 , or acetonitrile- d_3 using the residual signals of chloroform, CHD_2OD , or acetonitrile- d_2 as internal standards. ^{13}C spectra of Ru(II) complexes were not collected due to the rather low solubility of these compounds. Accurate mass measurements (ESI-HRMS) were performed with a Thermo Scientific Orbitrap Elite high-field orbitrap hybrid mass spectrometer. MALDI-TOF mass spectra were registered on a Bruker Daltonics Autoflex II mass spectrometer in the positive ion mode with a dithranol matrix and polyethyleneglycols as internal standards. FTIR spectra were registered on Nicolet iS 5 and Bruker Vector 22 spectrophotometers. Micro-ATR accessory (Pike) was used in order to register the FTIR spectra of polycrystalline solid complexes. The limit of detection (LOD) of Cu(II) ions was determined by UV–Vis and fluorescence spectroscopies using the 3σ method [30].

2.3. Synthesis

Synthetic procedures, characterization of the compounds, and their IR and NMR spectra are given in the Supplementary Materials.

2.4. Protonation and Complexation Studies

Protonation and complexation studies were performed at room temperature. The solutions were prepared with double-deionized high-purity water (18.2 $\text{M}\Omega$ cm) obtained from a Millipore Simplicity apparatus. Solution concentrations and other experiment conditions are given in the corresponding figures and tables. Protonation studies were conducted in a glass beaker equipped with magnetic stirrer and pH-electrode adding HCl (4 or 0.01 M) or KOH (5 or 0.01 M) to the solutions of complexes. Metal-binding experiments were conducted by a manual addition of the aliquots of metal salt solutions by a Hamilton syringe to a solution of chemosensor placed in a quartz cuvette. All metal salts used were perchlorates of general $\text{M}(\text{ClO}_4)_n \cdot x\text{H}_2\text{O}$ formula. *Caution: although no problems were experienced, perchlorate salts are potentially explosive when combined with organic ligands and should be manipulated with care and used only in very small quantities.*

The $\text{Hg}(\text{ClO}_4)_2$ solution was prepared in acetonitrile (HPLC, Merck) to avoid hydrolysis of the salt. Aqueous solutions of metal perchlorates were prepared with concentrations approximately 1000-fold of that of the ligands in order to decrease the influence of the medium changes on the spectra of the studied solutions. Stability constants were calculated using nonlinear least squares analysis by means of HYPERQUAD software [31] after factor

analysis of the combined data sets [32]. The goodness of fit was assessed through the scaled standard deviation of the residuals (s), which has an expectation value of unity in the absence of systematic errors assuming a correct weighting scheme. The results were checked by plotting calculated molar extinction graphs (Figure S15). The calculated species distribution diagram for the **Ru(N₂P₂phen)/Cu²⁺** system in water is shown in Figure S16.

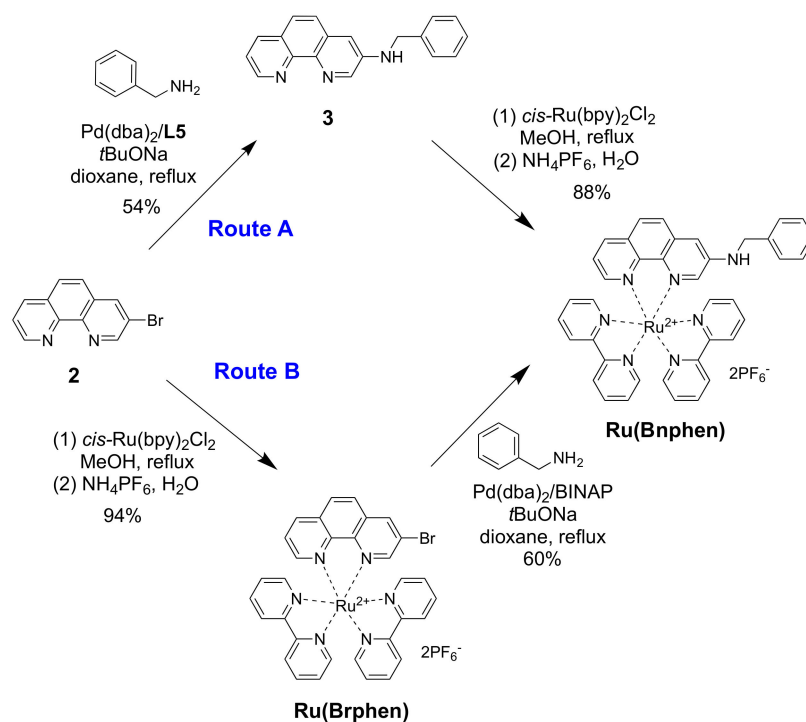
3. Results and Discussion

3.1. Synthesis

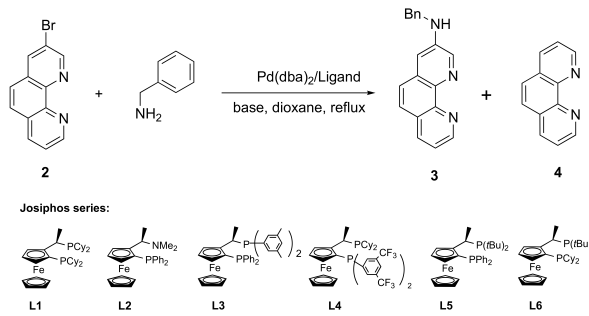
The molecular probe **Ru(N₂P₂phen)** can be obtained from available 3-bromo-1,10-phenanthroline (**2**) according to a three-step reaction sequence involving (i) the nucleophilic substitution of the bromine atom by a polyamine; (ii) the complexation of the phen chelator by *cis*-Ru(bpy)₂Cl₂; (iii) the *N*-alkylation of this compound by bromide **1**. These reactions can be performed in various orders (Scheme 2). The amination can be placed before (Routes A and C) or after (Route B) the complexation of the phen ligand by ruthenium(II). Moreover, the *N*-functionalization can occur before the complexation (Route C) or in the last step of the synthetic scheme (Routes A and B).

The substitution of the bromine atom of the 1,10-phenanthroline ring by a polyamine is a challenging step in all of these synthetic approaches due to the rather low reactivity of such bromides in the nucleophilic substitution reactions. Palladium or copper catalyst is often required to perform these reactions, but both 1,10-phenanthroline and polyamines are known to form stable complexes with these metals that can interrupt the catalytic cycle.

Preliminary experiments were performed using a more reactive and non-chelating primary amine, benzylamine (Scheme 3). The results of amination of 3-bromo-1,10-phenanthroline (**2**) (Route A, step 1) are summarized in Table 1.



Scheme 3. Synthesis of the aminophenanthroline-ruthenium complex **Ru(Bnphen)**.

Table 1. Amination of 3-bromo-1,10-phenanthroline (**2**) with benzylamine ¹.


Entry	Ligand	(Pd)/Ligand (mol %)	Base	Yield, % ²	
				3	4
1 ³	-	-	Cs ₂ CO ₃ ⁴	0 ⁵	0
2 ^{3,6}	-	-	Cs ₂ CO ₃ ⁴	0	100
3	BINAP ⁷	2/4	<i>t</i> BuONa	traces	100
4	BINAP ⁷	2/25	<i>t</i> BuONa	traces	100
5	BINAP ⁷	10/10.5	<i>t</i> BuONa	30 (28)	70
6	BINAP ⁷	10/10.5	<i>t</i> BuONa	30	70
7	BINAP ⁷	10/25	Cs ₂ CO ₃ ⁴	<15	85
8	BINAP ⁷	10/10.5	K ₃ PO ₄ ⁴	0	100
9 ⁸	BINAP ⁷	10/10.5	<i>t</i> BuONa	16	80
10	L1	10/10.5	<i>t</i> BuONa	35	60
11	L2	10/10.5	<i>t</i> BuONa	0	100
12	L3	10/10.5	<i>t</i> BuONa	35	65
13	L4	10/10.5	<i>t</i> BuONa	<15	85
14	L5	10/10.5	<i>t</i> BuONa	60 (54)	30
15	L6	10/10.5	<i>t</i> BuONa	60 (50)	30

¹ Reaction conditions: **2** (0.25 mmol), Pd(dba)₂, the ligand, and the base (1.5 equivalents) were vigorously stirred in dioxane (2.5 mL) at reflux for 16 h under inert atmosphere. A complete conversion of the starting bromide (NMR monitoring) was achieved in all experiments. ² Determined by NMR spectroscopy. The isolated yields are given in parenthesis. ³ The reaction was performed in DMF at 140 °C without addition of Pd(dba)₂. ⁴ Two equivalents of the base was used. ⁵ No conversion of the bromide was observed. ⁶ CuI (2 equivalents) was added instead of Pd(dba)₂. ⁷ 2,2'-bis(diphenylphosphino)-1,1'-binaphthyl. ⁸ Reaction was performed in toluene using 3 equivalents of amine.

As expected, compound **2** did not react with benzylamine in DMF at 140 °C (entry 1), in contrast to the more reactive 1,10-phenanthrolines bearing halogen substituents at positions 4 or 7, which do react with amines under these conditions [33,34]. Copper- and palladium-catalyzed amination of 3-bromo-1,10-phenanthroline (**2**) were reported, but only for a few nucleophiles with enhanced NH acidity such as imidazole, carbazole, phenoxazine, or diarylamines [35–38]. Addition of CuI [36,39] in the reaction under study afforded exclusively the dehalogenated product, phen (**4**) (entry 2). Catalysis with palladium complexes under standard conditions (Pd(dba)₂/BINAP, *t*BuONa, dioxane, and reflux) [40–44] also gave only this dehalogenated product (entry 3), and even a huge excess of ligand failed to suppress this reduction (entries 3 and 4), which is commonly observed as a side reaction in palladium-catalyzed C–N coupling [45,46]. Chelation of palladium with phen is likely to interfere, as it may hamper proper control of the coordination shell of the metal by the diphosphine ligand. Noteworthy is the fact that the more sterically hindered bromo-substituted 2,9-dimethyl-1,10-phenanthrolines in the reactions with primary amines did not cause such problems [47].

Meanwhile, increasing the Pd(dba)₂ loading up to 10 mol% resulted in the formation of target compound **3**, though only as a minor product in 28% yield (entry 5). Further experiments in which the base and the solvent were varied along with increasing amounts of the amine and BINAP failed to provide any essential improvements (entries 6–9). Among many ligands tested (listed in Tables 1 and S1), only some of the expensive ones belonging to

the Josiphos family, like **L5** and **L6**, afforded the desired coupling product **3** (entries 10–15) in reasonable yields (50–54%; Table 1, entries 14 and 15). Fortunately, further complexation of aminophenanthroline **3** to *cis*-Ru(bpy)₂Cl₂ was straightforward and gave the target complex **Ru(Bnphen)** in 88% yield (Scheme 3, Route A).

We also explored an alternative procedure (Route B in Scheme 3) consisting of the prior preparation of complex [Ru(Brphen)(bpy)₂](PF₆)₂ (**Ru(Brphen)**) followed by the amination reaction. In this case, the phen chelator could not compete with the diphosphine ligand in the catalytic cycle, as it was engaged in a stable Ru complex.

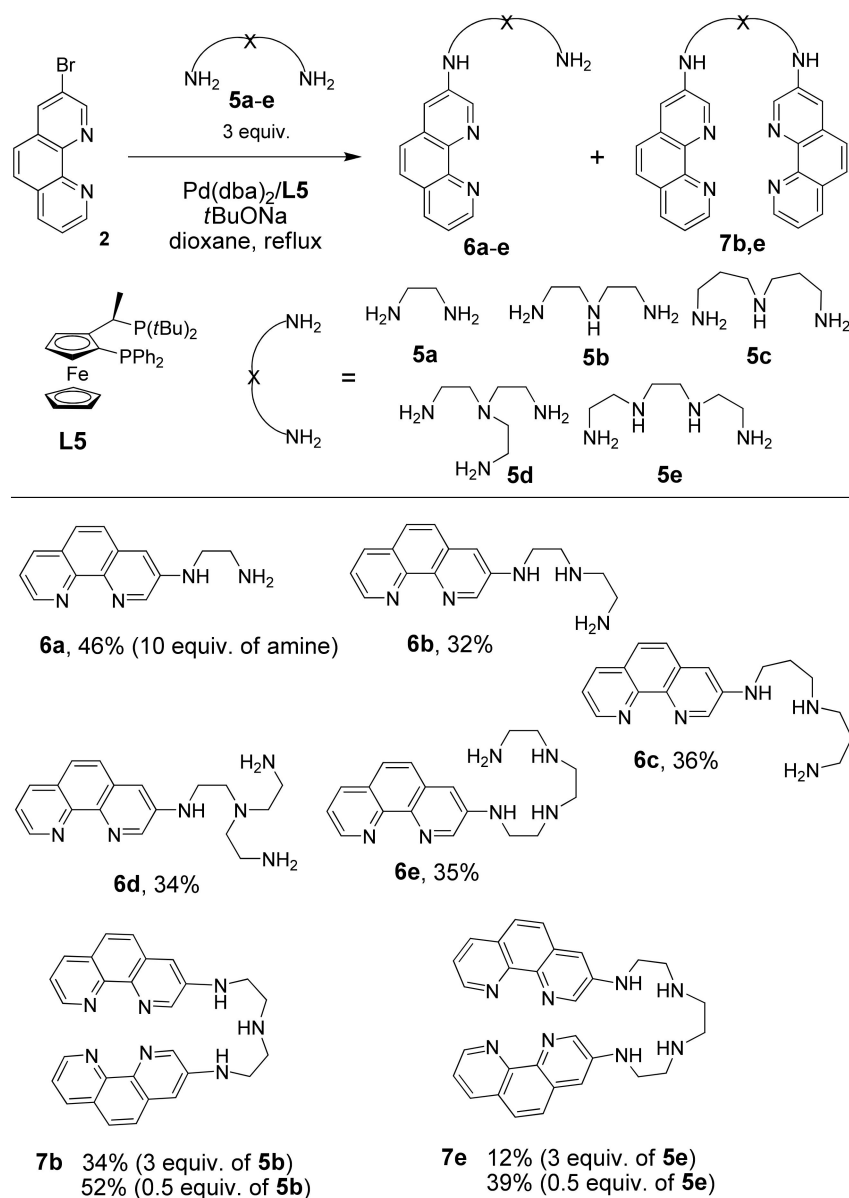
The **Ru(Brphen)** complex was prepared in 94% yield and introduced in the amination reaction with benzylamine using the relatively cheap Pd(dba)₂/BINAP catalytic system. This coupling was also accompanied by the reductive debromination leading to the [Ru(phen)(bpy)₂](PF₆)₂ complex. The target compound, **Ru(Bnphen)**, was isolated in 60% yield following this approach, which was twice as much as the yield obtained for the amination of bromide **2** using BINAP (Table 1, entry 5) and slightly better than the results obtained with the best **L5** and **L6** ligands (Table 1, entries 14 and 15). Nevertheless, the separation of the two highly polar complexes by column chromatography turned out to be laborious, especially in a scaled-up synthesis where the pure compounds were obtained only after three consecutive chromatographic runs. Thus, Route A, involving the amination of the ligand, was chosen for the preparation of polyamine derivatives.

Bromide **2** was reacted with unprotected polyamines because the reactions of linear primary and secondary polyamines with aryl halides are known to be chemoselective and lead to the *N*-functionalization of only the primary amino groups [48]. The catalytic reactions of bromide **2** by chelating polyamines **5a–e**, which differ by the number of nitrogen atoms and by length of the alkyl chains, were performed using the most efficient ligand, **L5**, by increasing the amount of the polyamines **5a–e** up to 3 equivalents (and even to 10 equivalents in the case of volatile diaminoethane **5a**) to diminish the consecutive coupling reactions leading to *N,N'*-bis(heteroaryl)-substituted products **7** (Scheme 4).

For all studied amines **5a–e**, the complete conversion of starting bromide **1** was achieved within 24 h when the reaction was performed with 10 mol% of Pd(dba)₂ and *t*BuONa in dioxane at reflux. However, the target products **6a–e** were isolated in only moderate yields (32–46%) due to the competing reduction and amination of the second primary amino group of **6a–e**, which produced polyamines **7**. To diminish the yields of bisheteroarylated products, the amount of starting polyamine **5b–e** was increased up to 5 equivalents. Unfortunately, separation of the product from an excess of polyamine was much more complicated under these conditions in comparison with the reactions described above, and several consecutive chromatographic columns were required resulting in product loss. Only for **6b** did we managed to increase the isolated yield up to 55% under these conditions.

Noteworthy was that the diarylated polyamines **7b** and **7e** could be obtained in good yields (52% and 39%, respectively) conducting the coupling reactions with 0.5 equivalents of the corresponding polyamines. This novel type of ambidentate bis(phenanthroline)–polyamine triads hold promise for development of sensors and supramolecular coordination polymers, which have recently attracted increasing interest [49].

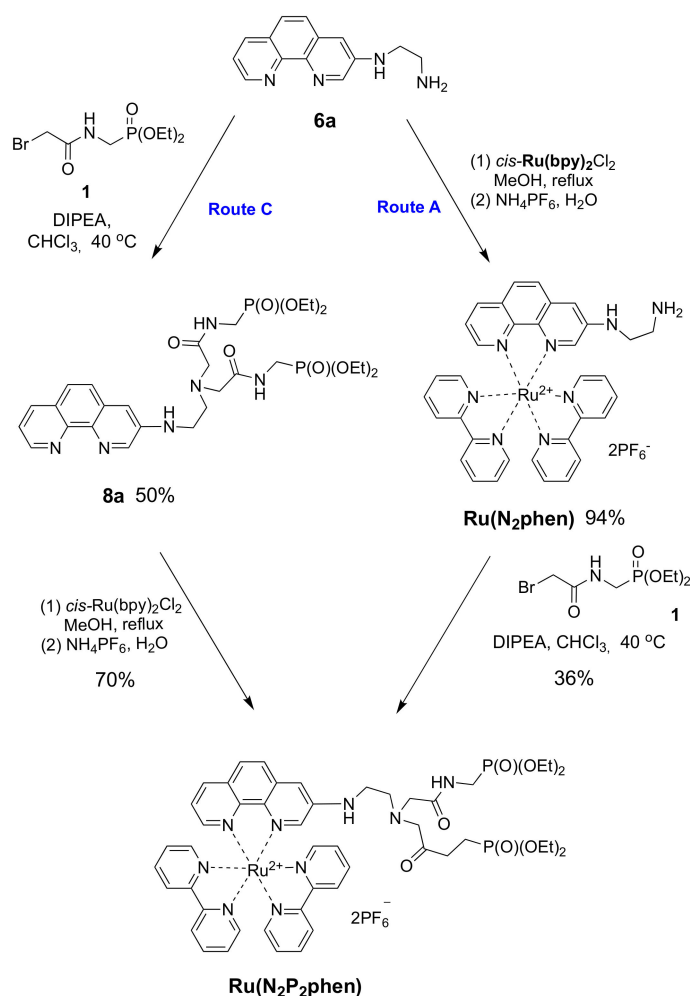
Next, the *N*-alkylation of amine **6a** with diethyl ((bromoacetyl)amino)methylphosphonate (**1**) was investigated. This reaction can also be performed using either the free chelator **6a** or the corresponding ruthenium(II) complex (Scheme 5). The *N*-alkylation of amines (Route C) is a classical method of synthesis, although it is well known for its rather poor selectivity and the undesired formation of quaternary ammonium salts due to the fact of overalkylation. Moreover, in our case, a competitive alkylation of the aromatic amino group was also observed as a side reaction. After optimization of the reaction conditions, the target product **8a** was obtained in 50% yield in chloroform at 40 °C using DIPEA as a base. The yield of **Ru(N₂P₂phen)** prepared from this chelator and *cis*-Ru(bpy)₂Cl₂ was only 70% due to the losses incurred from the high solubility of complex **8a** in all organic solvents and aqueous media.



Scheme 4. Pd-catalyzed synthesis of 1,10-phenanthroline-polyamine chelators **6a–e** and **7b,e**.

Therefore, we tried to increase the selectivity of the *N*-alkylation by conducting the reaction with the **Ru(N₂phen)** precursor, assuming a reduced nucleophilicity of the aromatic amino group compared to that exhibited by the free phenanthroline derivative as a consequence of electronic and steric effects (Route A). The complex **Ru(N₂phen)** was prepared in 71% yield by reacting phenanthroline **6a** with *cis*-(bpy)₂RuCl₂ before converting the reaction product with bromide **1** in the presence of DIPEA in chloroform. Unfortunately, the desired complex, **Ru(N₂P₂phen)**, was obtained in 36% yield only after tedious chromatographic purification.

Thus, the insertion of a metal atom at the last step (Route C, Scheme 1) was the least resource- and time-consuming procedure among those explored, though comparable product yields can be obtained using other routes. It is worth noting that this synthetic pathway can be readily adapted for the synthesis of various visible light-active transition metals (Ru^{II}, Ir^{III}, Re^{II}, Os^{II}, Fe^{II}, Co^{II}, and Pt^{II}), if screening of chromogenic molecular probes would be needed.



Scheme 5. Synthesis of chemosensor $\text{Ru}(\text{N}_2\text{P}_2\text{phen})$.

The examples of the functionalization of Ru^{2+} complexes reported in this work unambiguously demonstrate that synthetic strategies based on introduction of the target substituent in the pre-formed Ru^{2+} complexes (“chemistry-on-the-complex”) [50] are of limited scope and hardly applicable to the preparation of complexes bearing ligands with any polar functional groups if the chromatographic purification of target product is required in the synthesis. According to our experience, the synthetic post-modification of the already assembled Ru^{2+} precursor could be of practical use only when the involved transformations are selective enough to afford the desired ruthenium complex after its precipitation from the reaction mixtures.

3.2. Optical Properties of $\text{Ru}(\text{N}_2\text{phen})$ and $\text{Ru}(\text{N}_2\text{P}_2\text{phen})$

$\text{Ru}(\text{N}_2\text{phen})$ and $\text{Ru}(\text{N}_2\text{P}_2\text{phen})$ are soluble in water at pH 0.5–12 and in 0.03 M HEPES solution under physiological conditions (pH = 7.4). Their spectroscopic data in aqueous media are summarized in Table 2.

The electronic absorption spectra of both compounds in pure water were similar and typical for mixed ligand $\text{Ru}(\text{bpy})_2(\text{phen})$ -type complexes. For both compounds, the π - π^* ligand-centered electronic transitions gave rise to intense bands in the 250–300 nm range [51,52]. The spectra also displayed characteristic broad absorption bands in the visible region that were assigned to the overlapping spin-allowed metal-ligand charge transfer (MLCT) and to interligand bpy/phen-based charge transfer (LLCT) transitions. The shape of the visible absorption bands was more complicated than that observed for $[\text{Ru}(\text{bpy})_3](\text{PF}_6)_2$. Their broadening was likely the result of an increased number of MLCT

and LLCT transitions in these unsymmetrical heteroleptic complexes [23]. An additional absorption maximum appearing in the 300–350 nm region presumably corresponded to ligand-ligand π - π^* transitions involving bipyridine and the aminated phenanthroline ligands [53]. As shown in Table 2, all bands were quite intensive which is welcome in view of further use in optical sensing.

Similar to many related ruthenium complexes [54], **Ru(N₂phen)** and **Ru(N₂P₂phen)** are bright luminophores (Table 2). In aerated HEPES solutions, the emission spectrum for each complex showed a broad band extending over approximately the 500–700 nm range with a maximum at 601 nm. The shape of the absorption and emission bands as well as the quantum yields were concentration independent within the limits of the experimental method, which is indicative of the absence of significant aggregation in solution. The luminescence quantum yields of 4% and 3% for **Ru(N₂phen)** and **Ru(N₂P₂phen)**, respectively, are roughly the same as those reported elsewhere for the parent [Ru(bpy)₃]²⁺ chromophore in aqueous media (4.2%) [54] and aerated acetonitrile (3.2%) [55].

Table 2. Photophysical data for Ru(N₂phen) and Ru(N₂P₂phen).

Complex	λ_{abs} , nm (log ϵ) ¹	λ_{em} , nm	Φ , % ²	Brightness, B ($\lambda = 450$ nm), $\text{M}^{-1} \text{cm}^{-13}$
Ru(N₂phen)	285 (4.64)	601 ^b	4	396
	350 (4.07)			
	450 (3.99)			
Ru(N₂P₂phen)	285 (4.82)	601 ^b	3	415
	350 (4.30)			
	450 (4.10)			

¹ Molar extinction coefficients (ϵ) are expressed in $\text{M}^{-1} \text{cm}^{-1}$. ² Quantum yields were determined in 0.03 M HEPES aerated solutions (pH = 7.4) using [Ru(bpy)₃]²⁺ in aerated acetonitrile ($\Phi = 3.2\%$) as a standard ($\lambda_{\text{ex}} = 450$ nm) [55]. ³ $B = \Phi(\lambda) \epsilon(\lambda)$ [20].

Both of the complexes studied have proton sensitive sites at the periphery of phenanthroline ring. Such complexes attracted constant interest as potential working elements of pH sensors. A wide range of new applications with specific demands justifies the development of novel pH-sensing concepts. The complexes with bipyridine ligands bearing hydroxy, sulfonic, and carboxylic groups or involving pyridine, imidazole, or calix [4] arene residues were investigated as luminescent molecular probes of pH levels [56,57]. Some of them were also successfully used in the development of photochemical-sensing devices [58–60]. To our knowledge, the reported Ru(II) complexes with phenanthroline ligands bearing the proton sensitive sites are limited to coordination compounds with 5-amino- [61] and 4,7-dihydroxy-1,10-phenanthrolines [62]. While the emission of the first compound is almost independent of pH, the luminescence of the hydroxy-substituted derivative varied in a wide pH range that was used to develop optical pH sensor devices for pH measuring in an unusually broad range of acidity levels [58].

We briefly investigated the acid–base behavior of **Ru(N₂phen)** and **Ru(N₂P₂phen)** by performing UV–Vis and luminescence titrations of these complexes in the range of pH 1–12 (Figures 1 and S1–S8).

The protonation of the nitrogen atom separated from the light absorbing aromatic moiety by a saturated NCH₂CH₂ linker had a rather weak influence on the light absorption by the complexes **Ru(N₂phen)** and **Ru(N₂P₂phen)** despite the presence in the linker of the nitrogen atom directly bonded to chromogenic unit and capable of the intramolecular hydrogen binding of protonated sites. Surprisingly, in the electronic absorption spectra of both complexes, only the band with the maximum at 350 nm was progressively blue-shifted from 350 to 346 nm upon gradual addition of hydrochloric acid. In contrast, the bands presumably corresponding to the lowest-energy MLCT transitions in the visible region (400–550 nm) were almost independent on pH. Similar changes in electronic adsorption spectra were reported for {Ru(bpy)₂[4-(4-hydroxyphenyl)-2,2'-bipyridine]}(PF₆)₂ and tenta-

tively explained assuming that the pH-sensitive site is not attached to the ligand involved in formation of the ground and excited states [63]. To obtain deeper insight into the electronic properties of our complexes, basic DFT computations were performed (Figure 2).

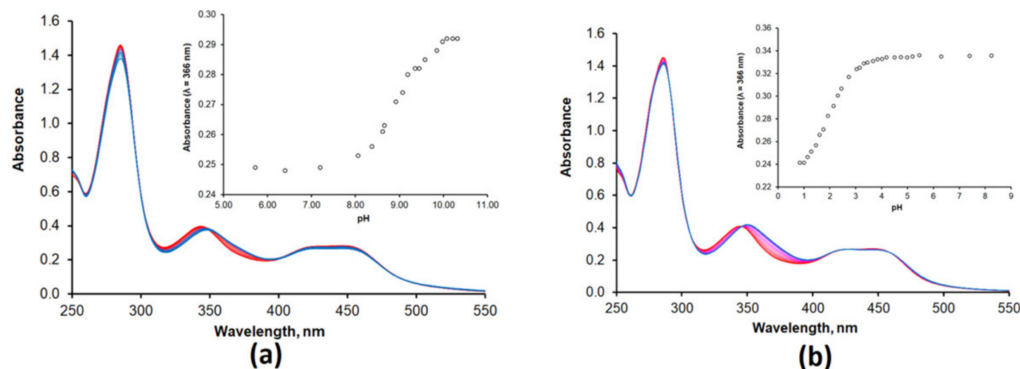


Figure 1. Evolution of the electronic absorption spectra of the compound **Ru(N₂phen)** ($[\text{Ru}(\text{N}_2\text{phen})]_{\text{tot}} = 33 \mu\text{M}$) (a) and **Ru(N₂P₂phen)** ($[\text{Ru}(\text{N}_2\text{P}_2\text{phen})]_{\text{tot}} = 21 \mu\text{M}$) (b) as a function of pH. The range of pH 1–12 was investigated for both complexes, but only the region of pH changing (see insets) are shown in the figure. Insets show the pH dependence of the absorbance at $\lambda_{\text{abs}} = 336 \text{ nm}$.

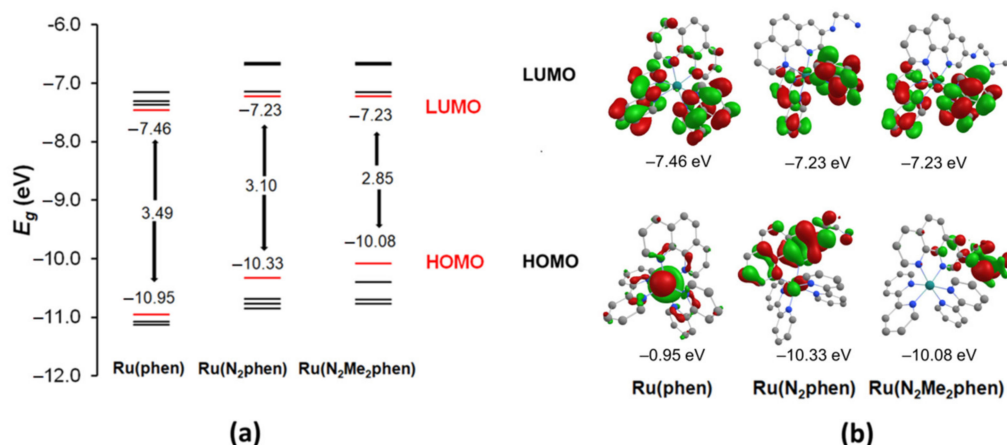


Figure 2. The schematic representation of the calculated energy levels in **Ru(phen)**, **Ru(N₂phen)**, and **Ru(N₂Me₂phen)** (a) and isodensity plots of the HOMO and LUMO orbitals for these complexes (b).

The DFT calculations with the Firefly quantum chemistry package [64], which is partially based on the GAMESS (US) [65] source code, were used to model the structure of the complexes. The B3LYP functional with the STO 6–31G(d,p) basis set was used in the calculations for all elements except ruthenium, for which the Stuttgart valence basis set and pseudopotential were employed [66]. The amidophosphonate fragment of **Ru(N₂P₂phen)** was replaced by a smaller methyl group and the corresponding complex was labeled **Ru(N₂Me₂phen)**. The optimized geometries of complexes **Ru(N₂phen)** and **Ru(N₂Me₂phen)** are depicted in Figures S20 and S21 (see Supplementary Materials). The metal atom had a distorted octahedral geometry and bonded to three chelate groups. The key structural parameters (i.e., Ru–N_{phen}, Ru–N_{bpy} bond length, and dihedral angles between ligand planes) of the chromogenic unit changed only slightly when alkyl substituents were introduced at the nitrogen atom of 1,10-phenanthroline ligand.

The isodensity plot of their HOMO and LUMO orbitals and the diagram showing their energy levels are shown in Figure 2 and compared to those of the parent complex $[\text{Ru}(\text{bpy})_2(\text{phen})]^{2+}$. Comparing the frontier orbitals of amino-substituted complexes to

those of parent **Ru(phen)**, one can notice that only in the last complex are both HOMO and HOMO₋₁ localized mainly on the Ru atom, while in other complexes the contribution of π orbitals of phen ligand is much more significant and dependent on the substitution pattern of the phenanthroline ring. The LUMO₀ and LUMO₊₁ orbitals of all complexes were constructed mainly of π orbitals of bipyridine ligands, and only LUMO₊₃ and LUMO₊₄ (not shown in Figure 2, see Tables S2 and S3) consisted of π orbitals of the aminophenanthroline ligand. Thus, the ligand to ligand charge transfer transition is supposed to give rise to intensive bands and can be red-shifted compared to the parent **Ru(phen)** complex. The absorption bands in the 340–360 nm region of the electronic absorption spectra of these complexes could correspond to MLCT transitions or an LL' transition with participation of the phenanthroline π orbitals. To obtain deeper insight into the studied question, correct modeling of the excited states of Ru²⁺ complexes is required, which can only be performed by sophisticated methods beyond the popular TD-DFT approach and, therefore, is beyond the scope of our work focusing on practical aspects of their use in analytic chemistry.

To determine the apparent protonation constants, numerical data fitting of spectrophotometric titration curves was performed using the HypSpec program (Figures S1–S3 and S5–S7) [30]. The best fits for both complexes were obtained when the UV–Vis titration data were processed with a single equilibrium model ($L + H^+ \rightleftharpoons LH^+$) that confirmed that the nitrogen atom directly linked to the phenanthroline ring cannot be protonated in aqueous medium. The refined values are collected in Table 3, together with the literature data for 1,2-diaminoethane (**5a**) [67] and the previously reported chemosensors **9** and **10** both bearing the same ionophore unit as the studied **Ru(N₂P₂phen)** (Figure 3) [68,69]. The distribution diagrams and electronic absorption spectra of the complexes, **Ru(N₂phen)** and **Ru(N₂P₂phen)**, and their monoprotonated forms calculated using the HypSpec program are shown in Figures S3 and S7, respectively.

Table 3. Apparent protonation constants or pK_a of **Ru(N₂phen)**, **Ru(N₂P₂phen)**, **5a**, **9**, and **10**¹.

Entry	Compound	pK_a	Reference
1	Ru(N₂phen)	9.13(7)	this work
2	5a	9.9–10.2 ² 6.8–7.5	[67]
3	Ru(N₂P₂phen)	2.02(1)	this work
4	9	2.26(1)	[68]
5	10	2.11(1)	[69]

¹ UV–Vis spectrophotometric measurements. $I = 0.1$ M KCl, $T = 298.2(2)$ K. ² The interval of the reported values are shown, see Reference [67].

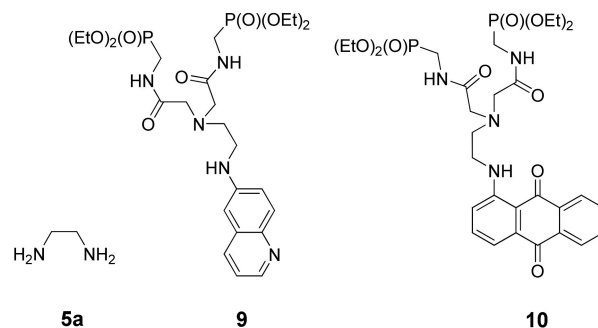


Figure 3. Structure of relevant compounds (i.e., **5a**, **9**, and **10**) for which protonation constants have been reported in the literature. The corresponding values are summarized in Table 3.

As it can be seen from Table 3, the protonation of **Ru(N₂phen)** and **Ru(N₂P₂phen)** occurs in separate pH ranges, in full agreement with the expected lower basicity of nitrogen atoms of **Ru(N₂P₂phen)** due to the presence of two electron-withdrawing substituents. It

is noteworthy that under physiological conditions, **Ru(N₂phen)** predominantly exists in the monoprotonated form while the polyamine chain of **Ru(N₂P₂phen)** is not protonated.

Comparing **Ru(N₂phen)** with 1,2-ethanediamine and **Ru(N₂P₂phen)** with dyes **9** and **10** bearing the same receptor unit (Figure 3), it can be concluded that the presence of a signaling group and its nature (organic vs. [Ru(bpy)₂(phen)]²⁺ chromophore) has only a weak influence on the acidity of the studied compounds, despite the positive charge of Ru(II)-based signaling group, which can be explained by separation of the protonated nitrogen atoms from this signaling group by aminoethylene linkers.

The emission of the complexes **Ru(N₂phen)** and **Ru(N₂P₂phen)** remained virtually constant over a wide pH range (pH = 0.5–10) (Figures S4 and S8). However, it diminished quickly and in a similar manner for both complexes in more basic solutions probably due to the fact of their partial decomposition under irradiation in the presence of strong bases, as it was already reported for the [Ru(bpy)₂(5-aminophenanthroline)](PF₆)₂ complex [61]. We assumed that the protonation of the polyamine chain had a negligible effect on the emission properties of the complexes due to the lack of efficient photoinduced electron transfer (PET) process from the side-chain amine groups to the [Ru(bpy)₂(phen)]²⁺ moiety as already reported for aliphatic amines and ruthenium–polypyridyl complexes [70]. It is noteworthy that this is in contrast to the behavior of the analogous compound **9** bearing the same polyamine chain attached to the 6-quinolinyl signaling group in which the protonation of the nitrogen atom leads to the increase in fluorescence intensity [68].

Thus, **Ru(N₂phen)** and **Ru(N₂P₂phen)** can be considered suitable dyes for spectroscopic monitoring of various analytes in aqueous media due to the fact of their high solubility and brightness. The low basicity of **Ru(N₂P₂phen)** is favorable for sensing metal ions at physiological pH (pH = 7.4), avoiding the competitive protonation of the ionophore under nearly neutral conditions.

3.3. Detection of Metal Cations in Solution

The sensing properties **Ru(N₂P₂phen)** were evaluated at a constant pH of 7.4 in HEPES buffered (c = 0.03 M) aqueous solutions. Firstly, UV–Vis absorption and emission spectra were recorded before and after the addition of 15 equivalents of 18 different metal perchlorate salts to the same **Ru(N₂P₂phen)** solution (Figures 4 and S10). Among all tested cations (i.e., Li⁺, Na⁺, K⁺, Mg²⁺, Ca²⁺, Sr²⁺, Ba²⁺, Mn²⁺, Fe²⁺, Co²⁺, Ni²⁺, Cu²⁺, Zn²⁺, Ag⁺, Cd²⁺, Hg²⁺, Pb²⁺, Al³⁺, and Cr³⁺), only Cu²⁺ induced an immediate change in the electronic absorption spectrum in the UV region (Figure S12), together with a partial but significant quenching of the luminescence (Figure 4) that could be detected instrumentally but also visually. The detection of Cu²⁺ ions, which are abundant in tap water and many food products, attracts considerable attention [71–74] due to the harmful effects of this metal on human health [75,76]. Sensing of Cu²⁺ by related [Ru(bpy–ionophore)(bpy)₂] complexes in which the signaling and receptor moieties are separated by an alkyl group was also investigated and led to the conclusion that emission quenching proceeds via the energy transfer rather than the electron transfer mechanism [77,78].

As shown in Figures 5a,b, S11 and S13, the competitive binding study revealed that Cu²⁺ could effectively be monitored in the presence of other metal ions including Co²⁺, Ni²⁺, Zn²⁺, Ag⁺, Cd²⁺, Hg²⁺, Pb²⁺, and Al³⁺.

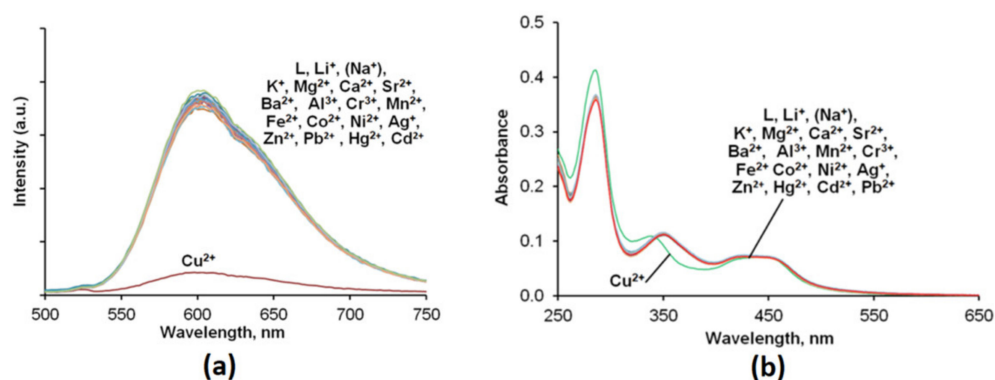


Figure 4. Fluorescence (a) and absorption spectra (b) of the $\text{Ru}(\text{N}_2\text{P}_2\text{phen})$ solution before and after addition of 15 equivalents of metal perchlorate salts. $[\text{Ru}(\text{N}_2\text{P}_2\text{phen})]_{\text{tot}} = 5.4 \mu\text{M}$, $\text{pH} = 7.4$, $[\text{HEPES}] = 0.03 \text{ M}$, and $[\text{M}^{n+}]_{\text{tot}} = 81.0 \mu\text{M}$ for each metal ion. $\lambda_{\text{ex}} = 450 \text{ nm}$.

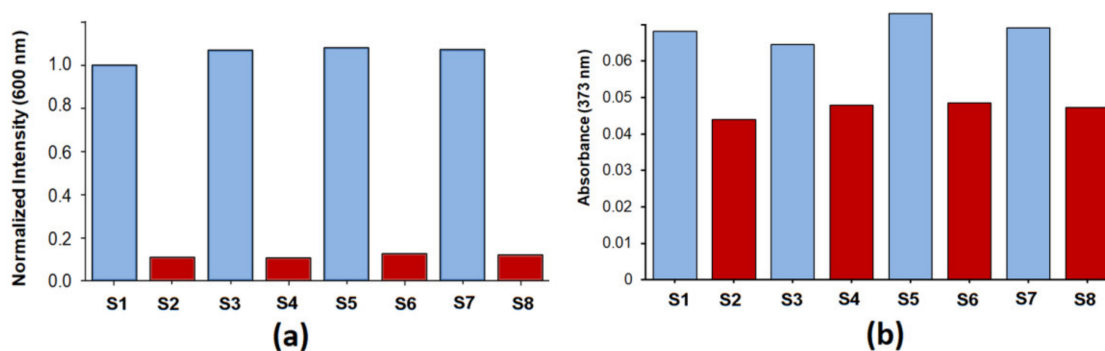


Figure 5. Cross-selectivity studies of metal ion binding by the ligand $\text{Ru}(\text{N}_2\text{P}_2\text{phen})$ ($[\text{Ru}(\text{N}_2\text{P}_2\text{phen})] = 5.4 \mu\text{M}$, $\text{pH} = 7.4$, $[\text{HEPES}] = 0.03 \text{ M}$, and $\lambda_{\text{ex}} = 450 \text{ nm}$) using fluorescence spectroscopy (a) and electronic absorption spectroscopy (b): (S1) intensity at 600 nm (a) and absorption at 326 nm (b) of the $\text{Ru}(\text{N}_2\text{P}_2\text{phen})$ solution; (S2) intensity at 600 nm (a) and absorption at 326 nm (b) of the $\text{Ru}(\text{N}_2\text{P}_2\text{phen})$ solution after addition of Cu^{2+} ($[\text{Cu}^{2+}]_{\text{tot}} = 81 \mu\text{M}$, 15 equivalents); (S3) intensity at 600 nm (a) and absorption at 326 nm (b) of the $\text{Ru}(\text{N}_2\text{P}_2\text{phen})$ solution after addition of Li^+ , (Na^+) , K^+ , Mg^{2+} , Ca^{2+} , Ba^{2+} , and Al^{3+} ($[\text{M}^{n+}]_{\text{tot}} = 81 \mu\text{M}$, 15 equivalents of each metal ion); (S4) spectrum of the $\text{Ru}(\text{N}_2\text{P}_2\text{phen})$ solution after addition of Li^+ , (Na^+) , K^+ , Mg^{2+} , Ca^{2+} , Ba^{2+} , Al^{3+} ($[\text{M}^{n+}]_{\text{tot}} = 81 \mu\text{M}$, 15 equivalents of each metal ion), and Cu^{2+} (15 equivalents); (S5) intensity at 600 nm (a) and absorption at 326 nm (b) of the $\text{Ru}(\text{N}_2\text{P}_2\text{phen})$ solution after addition of Mn^{2+} , Co^{2+} , Ni^{2+} , and Zn^{2+} ($[\text{M}^{n+}]_{\text{tot}} = 81 \mu\text{M}$, 15 equivalents of each metal ion); (S6) spectrum of the $\text{Ru}(\text{N}_2\text{P}_2\text{phen})$ solution after addition of Mn^{2+} , Co^{2+} , Ni^{2+} , Zn^{2+} ($[\text{M}^{n+}]_{\text{tot}} = 81 \mu\text{M}$, 15 equivalents of each metal ion), and Cu^{2+} ($[\text{Cu}^{2+}]_{\text{tot}} = 81 \mu\text{M}$, 15 equivalents); (S7) intensity at 600 nm (a) and absorption at 326 nm (b) of the $\text{Ru}(\text{N}_2\text{P}_2\text{phen})$ solution after addition of Ag^+ , Hg^{2+} , Cd^{2+} , and Pb^{2+} ($[\text{M}^{n+}]_{\text{tot}} = 81 \mu\text{M}$, 15 equivalents of each metal ion); (S8) intensity at 600 nm (a) and absorption at 326 nm (b) of the $\text{Ru}(\text{N}_2\text{P}_2\text{phen})$ solution after addition of Ag^+ , Hg^{2+} , Cd^{2+} , Pb^{2+} ($[\text{M}^{n+}]_{\text{tot}} = 81 \mu\text{M}$, 15 equivalents of each metal ion), and Cu^{2+} ($[\text{Cu}^{2+}]_{\text{tot}} = 81 \mu\text{M}$, 15 equivalents).

The selectivity did not change with time and can be explained by a higher affinity of $\text{Ru}(\text{N}_2\text{P}_2\text{phen})$ for Cu^{2+} compared to other metal ions. The titration experiments showed that the stability constant of the bimetallic $\{\text{Cu}[\text{Ru}(\text{N}_2\text{P}_2\text{phen})]\}^{4+}$ complex was as low as $\log \beta = 4.2$ (1), and more than 20 equivalents of copper are required to saturate the receptor (Figures 6 and S14).

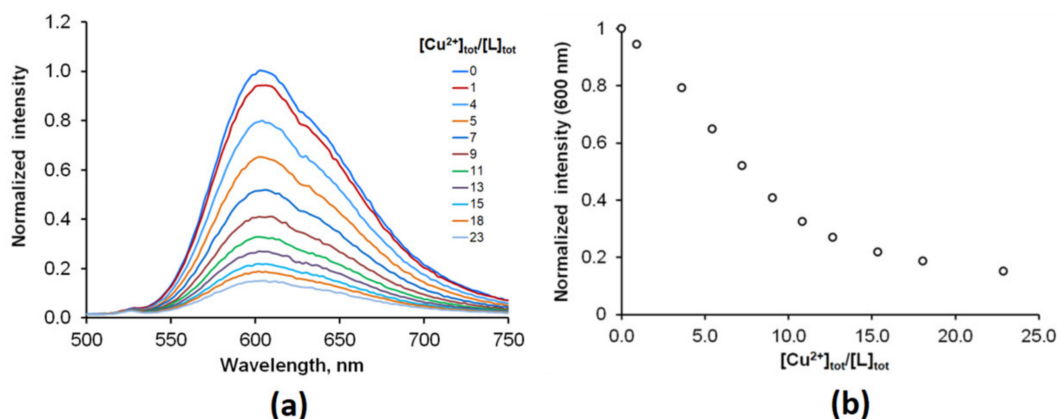


Figure 6. (a) Evolution of the fluorescence spectrum of the **Ru(N₂P₂phen)** solution upon addition of $\text{Cu}(\text{ClO}_4)_2$ (0–23 equivalents) ($[\text{Ru}(\text{N}_2\text{P}_2\text{phen})]_{\text{tot}} = 5.4 \mu\text{M}$, $\text{pH} = 7.4$, $[\text{HEPES}] = 0.03 \text{ M}$, $[\text{Cu}^{2+}]_{\text{tot}} = 0\text{--}128 \mu\text{M}$ and $\lambda_{\text{ex}} = 450 \text{ nm}$). (b) Changes in the fluorescence intensity with $[\text{Cu}^{2+}]_{\text{tot}}/[\text{Ru}(\text{N}_2\text{P}_2\text{phen})]_{\text{tot}}$ ratio at $\lambda_{\text{em}} = 600 \text{ nm}$. $[\text{Cu}^{2+}]_{\text{tot}}$ concentrations for each point: 1–0; 2–5.2; 3–20.7; 4–31.0; 5–41.3; 6–51.5; 7–61.7; 8–71.8; 9–86.9; 10–102.0; 11–128.0 μM .

However, with a detection limit (LOD) of 9 and 6 μM , as estimated by absorption and emission spectrophotometry, respectively, **Ru(N₂P₂phen)** can be used for the analysis of tap water, because the copper action level in drinking water is fixed at 20 μM by the US Environmental Protection Agency (US EPA) [79]. Interestingly, despite its rather low affinity to Cu^{2+} ion, the sensibility of **Ru(N₂P₂phen)** is comparable to other organic molecular probes, including chemosensors **9** [68] and **10** [69], as a consequence of its high brightness in aqueous media. It is also worth noting that chemosensors based on luminescent ruthenium tris(diimine) complexes have previously been reported, and some of them displayed lower detection limits [19,80–87].

Unfortunately, all our attempts to grow single crystals of the copper(II) complex of **Ru(N₂P₂phen)** failed. Hence, structural information on the complex was gained by combining UV–Vis, FTIR, and ESI-HRMS analyses of the sample prepared by the treatment of the **Ru(N₂P₂phen)** chemosensor with one equivalent of $\text{Cu}(\text{ClO}_4)_2$ in methanol and the evaporation of the solvent to dryness.

The ESI-HRMS signal corresponding to the $[\text{Cu}+\text{Ru}(\text{N}_2\text{P}_2\text{phen})-2\text{H}]^{2+}$ species confirmed the formation of 1:1 copper adduct (Figure S17). A hypsochromic shift of the absorption maximum observed for **Ru(N₂P₂phen)** after addition of Cu^{2+} ions in electronic absorption spectrum, presumably indicates that the coordination of the aromatic nitrogen atom to Cu^{2+} was observed under studied conditions.

Coordination of the amide groups was inferred from FTIR spectra collected in the 1500–1700 cm^{-1} region for $[\text{Cu}[\text{Ru}(\text{N}_2\text{P}_2\text{phen})]^{4+}$ and **Ru(N₂P₂phen)** (Figures S18 and S19). The amide I ($\nu_{\text{C}=\text{O}} = 1669\text{--}1671 \text{ cm}^{-1}$) and amide II ($\delta_{\text{C-NH}} = 1524\text{--}1531 \text{ cm}^{-1}$) bands of the ligands were present in the spectrum of **Ru(N₂P₂phen)** (Figure S18). The $\nu_{\text{C}=\text{O}}$ vibration energy is diagnostic for the extent of π -electron delocalization. The amide I band appears in the 1615–1625 cm^{-1} region when the carbonyl oxygen atom is bound to a metal [88], whereas coordination of the deprotonated nitrogen atom (the amidate binding mode) produces a red shift of the $\nu_{\text{C}=\text{O}}$ vibration mode down to $\sim 1580 \text{ cm}^{-1}$. In our case, the spectral interpretation is intricate owing to the overlap of several other bands in this region. Nevertheless, we can safely conclude that the $\nu_{\text{C}=\text{O}}$ stretching modes appear in the 1635–1590 cm^{-1} region, indicating that most probably the oxygen atom of the amide group is coordinated to the metal center (Figure 7).

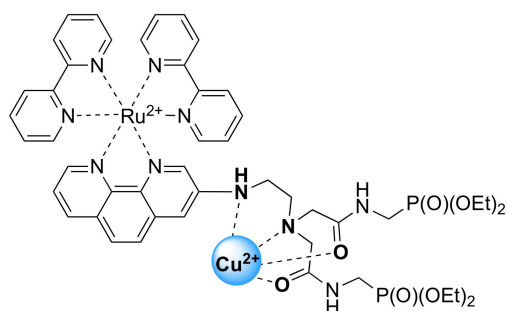


Figure 7. Schematic presentation of binding mode of **Ru(N₂P₂phen)** ligand in coordination shell of copper(II) ion.

The importance of the functionalization of the primary amine group for Cu²⁺ complex formation was demonstrated in comparative studies of Cu²⁺ binding by **Ru(N₂P₂phen)** and **Ru(N₂phen)** chelators. Both the UV–Vis and emission spectra of **Ru(N₂phen)** were insensitive to the presence of Cu²⁺ ions, even when these ions were present in the studied solution in large excess (30 equivalents), which indicates that the diaminoethylene residue of **Ru(N₂phen)** does not ligate any metal ions in aqueous media (Figure S9). The lower affinity of **Ru(N₂phen)** to Cu²⁺ ions compared to that of **Ru(N₂P₂phen)** can likely be explained by the protonation of its probably primary amine group at physiological pH (Table 2) and a decrease in the number of donor groups in the receptor unit. Thus, the electron-withdrawing amide groups may be expected to play a decisive role in the complexation of Cu²⁺ ions while the selectivity of this ligand probably resulted from a rather low metal affinity of diaminoethane fragment bearing heteroaromatic substituent (1,10-phenanthroline) at the nitrogen atom.

Ru(N₂P₂phen) would be suitable for the real-time dual-channel (UV–Vis absorption and fluorescence spectroscopies) analysis of tap water. It is noteworthy that most of the so far reported luminescent [Ru(diimine–ionophore)(diimine)₂] conjugates exhibited negligible changes in their electronic absorption properties upon addition of Cu²⁺ ions [19,80–87,89]. The markedly enhanced spectral response of **Ru(N₂P₂phen)** can be directly ascribed to the conjugation of the ionophore with the 1,10-phenanthroline core. Another important advantage of the newly synthesized chemosensor is the presence of the phosphonate anchoring groups that do not participate in the coordination of the copper atom (Figure 7) and can be used in developing photochemical sensing devices.

4. Conclusions

3-Polyamine-substituted 1,10-phenanthrolines are now available from commercial starting compounds in one step. These compounds were prepared by the selective Pd-catalyzed amination of 3-bromo-1,10-phenanthroline by PAs. These ditopic ligands are of interest for developing bimetallic supramolecular polymers and molecular probes. In this work, synthetic approaches to their Ru²⁺ complexes were investigated to prepare emissive complexes for sensing applications. We also demonstrated using **Ru(N₂phen)** as a representative example that parent Ru²⁺ complexes bearing PA receptors can be modified by diethyl ((bromoacetyl amino)methyl)phosphonate to obtain water-soluble molecular probes. The target complex **Ru(N₂P₂phen)** was also prepared using a stepwise modification of [Ru(bpy)₂(**Brphen**)](PF₆)₂ to compare “chemistry-on-the-complex” and “chemistry-on-the-ligand” synthetic approaches. These studies demonstrated that the functionalization of ligands is more convenient in the synthesis of Ru²⁺ complexes with hydrophilic functional groups.

The optical and sensing properties of the water-soluble **Ru(N₂P₂phen)** complex were investigated and compared to those of the parent **Ru(N₂phen)**. The **Ru(N₂P₂phen)** complex allows for selective double-channel detection of the Cu²⁺ ion at physiological pH by monitoring simultaneously the absorption changes and the phosphorescence turn-off

(ON–OFF probe) of the test solution. Among all tested cations (i.e., Li^+ , Na^+ , K^+ , Mg^{2+} , Ca^{2+} , Sr^{2+} , Ba^{2+} , Mn^{2+} , Fe^{2+} , Co^{2+} , Ni^{2+} , Cu^{2+} , Zn^{2+} , Ag^+ , Cd^{2+} , Hg^{2+} , Pb^{2+} , Al^{3+} , and Cr^{3+}), only Cu^{2+} induced an immediate change in the electronic absorption spectrum in the UV region, together with a partial but significant quenching of the luminescence that could be detected instrumentally but also visually. The LOD of Cu^{2+} , determined by spectrophotometry and fluorescence spectroscopy, was equal to 9 and 6 μM , respectively. The importance of functionalization of the primary amine group for sensing was demonstrated in comparative studies of Cu^{2+} binding by **Ru(N₂P₂phen)** and **Ru(N₂phen)** chelators. **Ru(N₂P₂phen)** can be used for the analysis of tap water and hold promise in the development of photochemical sensing devices due to the presence at the periphery of the phenanthroline ligand of two phosphonate anchoring groups.

Supplementary Materials: The following supporting information can be downloaded at: <https://www.mdpi.com/article/10.3390/chemosensors10020079/s1>, Synthetic procedures, Figure S1: Spectrophotometric titration of **Ru(N₂phen)** ($[\text{Ru}(\text{N}_2\text{phen})] = 33 \mu\text{M}$, $I = 0.1 \text{ M KCl}$, $\text{pH} = 5.7\text{--}11.6$), Figure S2: Absorbance changes with pH at $\lambda = 367 \text{ nm}$ for **Ru(N₂phen)**, Figure S3: (a) UV–vis spectra of **Ru(N₂phen)** and $[\text{Ru}(\text{N}_2\text{phen})\text{H}]^+$ in water calculated using Hyperquad program [31]. (b) Species distribution diagram for the **Ru(N₂phen)/H⁺** system in water calculated using Hyperquad program [31], Figure S4: Fluorimetric titration of **Ru(N₂phen)** ($[\text{Ru}(\text{N}_2\text{phen})] = 11 \mu\text{M}$, $I = 0.1 \text{ M KCl}$, $\lambda_{\text{ex}} = 450 \text{ nm}$, $\text{pH} = 5.7\text{--}10.5$), Figure S5: Spectrophotometric titration of **Ru(N₂P₂phen)** ($[\text{Ru}(\text{N}_2\text{P}_2\text{phen})] = 21 \mu\text{M}$, $I = 0.1 \text{ M KCl}$, $\text{pH} = 1.0\text{--}9.2$), Figure S6: Absorbance changes with pH at $\lambda = 330 \text{ nm}$ for **Ru(N₂P₂phen)**, Figure S7: (a) UV–vis spectra of **Ru(N₂P₂phen)** and $[\text{Ru}(\text{N}_2\text{P}_2\text{phen})\text{H}]^+$ in water calculated using Hyperquad program [31]. (b) Species distribution diagram for the **Ru(N₂P₂phen)/H⁺** system in water calculated using Hyperquad program [31], Figure S8: Fluorimetric titration of **Ru(N₂P₂phen)** ($[\text{Ru}(\text{N}_2\text{P}_2\text{phen})] = 6.6 \mu\text{M}$, $I = 0.1 \text{ M KCl}$, $\lambda_{\text{ex}} = 450 \text{ nm}$, $\text{pH} = 1.1\text{--}9.3$), Figure S9: Evolution of fluorescence spectrum of **Ru(N₂phen)** upon addition of $\text{Cu}(\text{ClO}_4)_2$ (0–30 equivalents) ($[\text{Ru}(\text{N}_2\text{phen})] = 11 \mu\text{M}$, $0.03\text{M HEPES buffer}$, $\text{pH} = 7.4$, $\lambda_{\text{ex}} = 450 \text{ nm}$), Figure S10: Fluorescence spectra of **Ru(N₂P₂phen)** ($[\text{Ru}(\text{N}_2\text{P}_2\text{phen})] = 5.4 \mu\text{M}$, $0.03\text{M HEPES buffer}$, $\text{pH} = 7.4$, $\lambda_{\text{ex}} = 450 \text{ nm}$) before and after addition of 15 equivalents of metal perchlorates ($[\text{M}^{n+}]_{\text{tot}} = 81 \mu\text{M}$ for each metal ion); (b) Normalized fluorescence intensity of the studied solutions at $\lambda_{\text{em}} = 600 \text{ nm}$, Figure S11: Cross-selectivity studies of metal ion binding by ligand **Ru(N₂P₂phen)** ($[\text{Ru}(\text{N}_2\text{P}_2\text{phen})] = 5.4 \mu\text{M}$, $0.03\text{M HEPES buffer}$, $\text{pH} = 7.4$, $\lambda_{\text{ex}} = 450 \text{ nm}$) using fluorescence spectroscopy: (S1) emission spectrum of **Ru(N₂P₂phen)**; (S2) emission spectrum of **Ru(N₂P₂phen)** after addition of Cu^{2+} (15 equivalents, $[\text{Cu}^{2+}]_{\text{tot}} = 81 \mu\text{M}$); (S3) emission spectrum of **Ru(N₂P₂phen)** after addition of Li^+ , (Na^+), K^+ , Mg^{2+} , Ca^{2+} , Ba^{2+} , Al^{3+} ($[\text{M}^{n+}]_{\text{tot}} = 81 \mu\text{M}$, 15 equivalents of each metal ion); (S4) emission spectrum of **Ru(N₂P₂phen)** after addition of Li^+ , (Na^+), K^+ , Mg^{2+} , Ca^{2+} , Ba^{2+} , Al^{3+} ($[\text{M}^{n+}]_{\text{tot}} = 81 \mu\text{M}$, 15 equivalents of each metal ion) and Cu^{2+} ($[\text{Cu}^{2+}]_{\text{tot}} = 81 \mu\text{M}$, 15 equivalents); (S5) emission spectrum of **Ru(N₂P₂phen)** after addition of Mn^{2+} , Co^{2+} , Ni^{2+} , Zn^{2+} ($[\text{M}^{n+}]_{\text{tot}} = 81 \mu\text{M}$, 15 equivalents of each metal ion); (S6) emission spectrum of **Ru(N₂P₂phen)** after addition of Mn^{2+} , Co^{2+} , Ni^{2+} , Zn^{2+} ($[\text{M}^{n+}]_{\text{tot}} = 81 \mu\text{M}$, 15 equivalents of each metal ion) and Cu^{2+} (15 equivalents, $[\text{Cu}^{2+}]_{\text{tot}} = 81 \mu\text{M}$); (S7) emission spectrum of **Ru(N₂P₂phen)** after addition of Ag^+ , Hg^{2+} , Cd^{2+} , Pb^{2+} ($[\text{M}^{n+}]_{\text{tot}} = 81 \mu\text{M}$, 15 equivalents of each metal ion) and Cu^{2+} (15 equivalents, $[\text{Cu}^{2+}]_{\text{tot}} = 81 \mu\text{M}$), Figure S12: (a) Absorption spectra of **Ru(N₂P₂phen)** ($[\text{Ru}(\text{N}_2\text{P}_2\text{phen})] = 5.4 \mu\text{M}$, $0.03\text{M HEPES buffer}$, $\text{pH} = 7.4$) before and after addition of 15 equivalents of metal perchlorates ($[\text{M}^{n+}]_{\text{tot}} = 81 \mu\text{M}$); (b) Absorbance of the studied solutions at $\lambda = 380 \text{ nm}$, Figure S13: Cross-selectivity studies of metal ion binding by ligand **Ru(N₂P₂phen)** ($[\text{Ru}(\text{N}_2\text{P}_2\text{phen})] = 5.4 \mu\text{M}$, $0.03\text{M HEPES buffer}$, $\text{pH} = 7.4$) using UV–vis spectroscopy: (S1) emission spectrum of **Ru(N₂P₂phen)**; (S2) emission spectrum of **Ru(N₂P₂phen)** after addition of Cu^{2+} ($[\text{Cu}^{2+}]_{\text{tot}} = 81 \mu\text{M}$, 15 equivalents); (S3) emission spectrum of **Ru(N₂P₂phen)** after addition of Li^+ , (Na^+), K^+ , Mg^{2+} , Ca^{2+} , Ba^{2+} , Al^{3+} ($[\text{M}^{n+}]_{\text{tot}} = 81 \mu\text{M}$, 15 equivalents of each metal ion); (S4) emission spectrum of **Ru(N₂P₂phen)** after addition of Li^+ , (Na^+), K^+ , Mg^{2+} , Ca^{2+} , Ba^{2+} , Al^{3+} ($[\text{M}^{n+}]_{\text{tot}} = 81 \mu\text{M}$, 15 equivalents of each metal ion) and Cu^{2+} ($[\text{Cu}^{2+}]_{\text{tot}} = 81 \mu\text{M}$, 15 equivalents); (S5) emission spectrum of **Ru(N₂P₂phen)** after addition of Mn^{2+} , Co^{2+} , Ni^{2+} , Zn^{2+} ($[\text{M}^{n+}]_{\text{tot}} = 81 \mu\text{M}$, 15 equivalents of each metal ion); (S6) emission spectrum of **Ru(N₂P₂phen)** after addition of Mn^{2+} , Co^{2+} , Ni^{2+} , Zn^{2+} ($[\text{M}^{n+}]_{\text{tot}} = 81 \mu\text{M}$, 15 equivalents of each metal ion) and Cu^{2+} ($[\text{Cu}^{2+}]_{\text{tot}} = 81 \mu\text{M}$, 15 equivalents);

(S7) emission spectrum of **Ru(N₂P₂phen)** after addition of Ag⁺, Hg²⁺, Cd²⁺, Pb²⁺ ([Mⁿ⁺]_{tot} = 81 μM, 15 equivalents of each metal ion); (S8) emission spectrum of **Ru(N₂P₂phen)** after addition of Ag⁺, Hg²⁺, Cd²⁺, Pb²⁺ ([Mⁿ⁺]_{tot} = 81 μM, 15 equivalents of each metal ion) and Cu²⁺ ([Cu²⁺]_{tot} = 81 μM, 15 equivalents), Figure S14: (a) Evolution of UV–vis spectrum of **Ru(N₂P₂phen)** upon addition of Cu(ClO₄)₂ (0–18) equivalents) ([**Ru(N₂P₂phen)**] = 5.6 μM, 0.03M HEPES buffer, pH = 7.4). (b) Changes of absorbance with [Cu²⁺]_{tot}/[**Ru(N₂P₂phen)**]_{tot} ratio at λ = 326 nm upon addition of Cu(ClO₄)₂ (0–18), Figure S15: (a) UV–vis spectra of **Ru(N₂P₂phen)²⁺** and [**Ru(N₂P₂phen)**Cu]⁴⁺ in water calculated using Hyperquad program [31], Figure S16: Species distribution diagram for the **Ru(N₂P₂phen)/Cu²⁺** system in water calculated using Hyperquad program [31] (Model for calculation: L ⇌ LH⁺; Cu²⁺ + L ⇌ [CuL]²⁺; Cu²⁺ ⇌ Cu(OH)⁺ ⇌ Cu₂(OH)₂²⁺ ⇌ Cu(OH)₂), Figure S17: HRMS (ESI) spectrum of the {Cu[**Ru(N₂P₂phen)**]}(ClO₄)₂ complex, Figure S18: FTIR spectrum of **Ru(N₂P₂phen)** (neat), Figure S19: FTIR spectrum of complex {Cu[**Ru(N₂P₂phen)**]}(ClO₄)₂ (neat), Figure S20: The structure of **Ru(N₂phen)** complex obtained by full geometry optimization at B3LYP/6-31G(d,p) level, Figure S21: The structure of **Ru(N₂Me₂phen)** complex obtained by full geometry optimization at B3LYP/6-31G(d,p) level, Figures S22–S45: NMR spectra of new compounds, Figure S46: FTIR spectrum of **Ru(Bnphen)** (neat), Figure S47: FTIR spectrum of **Ru(N₂phen)** (neat); Table S1: Optimization of the amination reaction conditions, Table S2: Calculated isodensity plot of the HOMO and LUMO orbitals for complex **Ru(N₂phen)**, Table S3: Calculated isodensity plot of the HOMO and LUMO orbitals for complex **Ru(N₂Me₂phen)**.

Author Contributions: Conceptualization, A.B.-L. and I.P.B.; Methodology, A.S.A.; Investigation, A.S.A., A.V.C. and A.D.A.; Writing—Original draft preparation, A.S.A.; Writing—Review and editing, A.B.-L., M.M. and A.S.A.; Visualization, A.S.A.; Project administration, A.B.-L. and A.D.A.; Funding acquisition, A.B.-L., A.S.A. and I.P.B. All authors have read and agreed to the published version of the manuscript.

Funding: This work was supported by the Russian Foundation for Basic Research (grant no. 18-33-00279). Financial support from the CNRS, the Conseil Régional de Bourgogne (PARI I ME SMT8 and PARI II CDEA programs), and the European Regional Development Fund (FEDER) is also acknowledged. A.S.A. is grateful to the French government and French embassy in Russia for the SSTE-2016 grant. This work was carried out in the frame of the International Associated French–Russian Laboratory of Macrocyclic Systems and Related Materials (LIA LAMREM) of CNRS and RAS (2011–2019).

Institutional Review Board Statement: Not applicable.

Informed Consent Statement: Not applicable.

Data Availability Statement: Not applicable.

Acknowledgments: Quentin Bonnin, Penouilh Marie-José, Diana Del Bianco, and Marcel Soustelle are warmly acknowledged for their technical support.

Conflicts of Interest: The authors declare no conflict of interest.

References

1. Santos, J.L.; Farahi, F. (Eds.) *Handbook of Optical Sensors*; CRC Press: Boca Raton, FL, USA, 2014; 718p.
2. Gunnlaugsson, T.; Leonard, J.P.; Murray, N.S. Highly selective colorimetric naked-eye Cu(II) detection using an Azobenzene Chemosensor. *Org. Lett.* **2004**, *6*, 1557–1560. [[CrossRef](#)] [[PubMed](#)]
3. Kaur, N.; Kumar, S. A diamide–diamine based Cu²⁺ chromogenic sensor for highly selective visual and spectrophotometric detection. *Tetrahedron Lett.* **2006**, *47*, 4109–4112. [[CrossRef](#)]
4. Ranyuk, E.; Douaihy, C.M.; Bessmertnykh, A.; Denat, F.; Averin, A.; Beletskaya, I.; Guilard, R. Diaminoanthraquinone-linked polyazamacrocycles: Efficient and simple colorimetric sensor for lead ion in aqueous solution. *Org. Lett.* **2009**, *11*, 987–990. [[CrossRef](#)] [[PubMed](#)]
5. Wang, X.-D.; Wolfbeis, O.S. Optical methods for sensing and imaging oxygen: Materials, spectroscopies and applications. *Chem. Soc. Rev.* **2014**, *43*, 3666–3761. [[CrossRef](#)] [[PubMed](#)]
6. Zhang, R.; Ye, Z.; Wang, G.; Zhang, W.; Yuan, J. Development of a ruthenium(II) complex based luminescent probe for imaging nitric oxide production in living cells. *Chem. Eur. J.* **2010**, *16*, 6884–6891. [[CrossRef](#)]
7. Park, H.-J.; Chung, Y.K. Ru(II)–M(I) (M = Rh and Ir) bimetallic complexes based on a bridging ligand composed of 1,10-phenanthroline and N-heterocyclic carbene: Coordination chemistry and detection property of carbon monoxide. *Inorg. Chim. Acta* **2012**, *391*, 105–113. [[CrossRef](#)]

8. Zhang, R.; Yu, X.; Ye, Z.; Wang, G.; Zhang, W.; Yuan, J. Turn-on luminescent probe for cysteine/homocysteine based on a ruthenium(II) complex. *Inorg. Chem.* **2010**, *49*, 7898–7903. [[CrossRef](#)]
9. Gill, M.R.; Thomas, J.A. Ruthenium(II) polypyridyl complexes and DNA—From structural probes to cellular imaging and therapeutics. *Chem. Soc. Rev.* **2012**, *41*, 3179–3192. [[CrossRef](#)]
10. Zhang, W.; Zhang, F.; Wang, Y.-L.; Song, B.; Zhang, R.; Yuan, J. Red-emitting ruthenium(II) and iridium(III) complexes as phosphorescent probes for methylglyoxal in vitro and in vivo. *Inorg. Chem.* **2017**, *56*, 1309–1318. [[CrossRef](#)]
11. Zhao, Q.; Li, F.; Huang, C. Phosphorescent chemosensors based on heavy-metal complexes. *Chem. Soc. Rev.* **2010**, *39*, 3007–3030. [[CrossRef](#)]
12. Mondal, D.; Bar, M.; Mukherjee, S.; Baitalik, S. Design of Ru(II) complexes based on anthraimidazoledione-functionalized terpyridine ligand for improvement of room-temperature luminescence characteristics and recognition of selective anions: Experimental and DFT/TD-DFT study. *Inorg. Chem.* **2016**, *55*, 9707–9724. [[CrossRef](#)]
13. Padilla-Tosta, M.E.; Lloris, J.M.; Martínez-Mañez, R.; Benito, A.; Soto, J.; Pardo, T.; Miranda, M.A.; Marcos, M.D. Bis(terpyridyl)-ruthenium(II) units attached to polyazacycloalkanes as sensing fluorescent receptors for transition metal ions. *Eur. J. Inorg. Chem.* **2000**, *2000*, 741–748. [[CrossRef](#)]
14. Watanabe, S.; Ikishima, S.; Matsuo, T.; Yoshida, K. A Luminescent metalloceptor exhibiting remarkably high selectivity for Mg^{2+} over Ca^{2+} . *J. Am. Chem. Soc.* **2001**, *123*, 8402–8403. [[CrossRef](#)]
15. Yue, Y.; Huo, F.; Cheng, F.; Zhu, X.; Mafireyi, T.; Strongin, R.M.; Yin, C. Functional synthetic probes for selective targeting and multi-analyte detection and imaging. *Chem. Soc. Rev.* **2019**, *48*, 4155–4177. [[CrossRef](#)]
16. Wang, J.-N.; Qi, Q.; Zhang, L.; Li, S.-H. Turn-on luminescent sensing of metal cations via quencher displacement: Rational design of a highly selective chemosensor for chromium(III). *Inorg. Chem.* **2012**, *51*, 13103–13107. [[CrossRef](#)] [[PubMed](#)]
17. Ru, J.; Mi, X.; Guan, L.; Tang, X.; Ju, Z.; Zhang, G.; Wang, C.; Liu, W. Design and application of a water-soluble phosphorescent Ru(II) complex as turn-on sensing material for Hg^{2+} . *J. Mater. Chem. B* **2015**, *3*, 6205–6212. [[CrossRef](#)] [[PubMed](#)]
18. Chen, F.; Xiao, F.; Zhang, W.; Lin, C.; Wu, Y. Highly stable and NIR luminescent Ru-LPMSN hybrid materials for sensitive Detection of Cu^{2+} in vivo. *ACS Appl. Mater. Interfaces* **2018**, *10*, 26964–26971. [[CrossRef](#)]
19. Kumar, S.; Arora, A.; Kaushal, J.; Oswal, P.; Kumar, A.; Kumar, P. Developing a simple and water soluble thiophene-functionalized Ru(II)-polypyridyl complex for ferric ion detection. *Inorg. Chem. Commun.* **2019**, *107*, 107500. [[CrossRef](#)]
20. Wong, K.-L.; Bünzli, J.-C.G.; Tanner, P.A. Quantum yield and brightness. *J. Lumin.* **2020**, *224*, 117256. [[CrossRef](#)]
21. Li, M.-J.; Chu, B.W.-K.; Zhu, N.; Yam, V.W.-W. Synthesis, structure, photophysics, electrochemistry, and ion-binding studies of ruthenium(II) 1,10-phenanthroline complexes containing thia-, seleno-, and aza-crown pendants. *Inorg. Chem.* **2007**, *46*, 720–733. [[CrossRef](#)]
22. Schmittel, M.; Lin, H.-W. Quadruple-channel sensing: A molecular sensor with a single type of receptor site for selective and quantitative multi-ion analysis. *Angew. Chem. Int. Ed.* **2007**, *46*, 893–896. [[CrossRef](#)] [[PubMed](#)]
23. Curtright, A.E.; McCusker, J.K. Static and time-resolved spectroscopic studies of low-symmetry Ru(II) polypyridyl complexes. *J. Phys. Chem. A* **1999**, *103*, 7032–7041. [[CrossRef](#)]
24. Abel, A.S.; Zenkov, I.S.; Averin, A.D.; Cheprakov, A.V.; Bessmertnykh-Lemeune, A.G.; Orlinson, B.S.; Beletskaya, I.P. Tuning the luminescent properties of ruthenium(II) amino-1,10-phenanthroline complexes by varying the position of the amino group on the heterocycle. *ChemPlusChem* **2019**, *84*, 498–503. [[CrossRef](#)] [[PubMed](#)]
25. Kálmán, F.K.; Woods, M.; Caravan, P.; Jurek, P.; Spiller, M.; Tircsó, G.; Király, R.; Brücher, E.; Sherry, A.D. Potentiometric and relaxometric properties of a gadolinium-based MRI contrast agent for sensing tissue pH. *Inorg. Chem.* **2007**, *46*, 5260–5270. [[CrossRef](#)]
26. Ukai, T.; Kawazura, H.; Ishii, Y.; Bonnet, J.J.; Ibers, J.A. Chemistry of dibenzylideneacetone-palladium(0) complexes: I. Novel tris(dibenzylideneacetone)dipalladium(solvent) complexes and their reactions with quinones. *J. Organomet. Chem.* **1974**, *65*, 253–266. [[CrossRef](#)]
27. Tzalis, D.; Tor, Y.; Salvatorre, F.; Jay Siegel, S. Simple one-step synthesis of 3-bromo- and 3,8-dibromo-1,10-phenanthroline: Fundamental building blocks in the design of metal chelates. *Tetrahedron Lett.* **1995**, *36*, 3489–3490. [[CrossRef](#)]
28. Lay, P.A.; Sargeson, A.M.; Taube, H.; Chou, M.H.; Creutz, C. *Cis*-bis(2,2'-bipyridine-*N,N'*) complexes of ruthenium(III)/(II) and osmium(III)/(II). *Inorg. Synth.* **1986**, *24*, 291–299. [[CrossRef](#)]
29. Albert, M.B. Standards for photoluminescence quantum yield measurements in solution (IUPAC Technical Report). *Pure Appl. Chem.* **2011**, *83*, 2213–2228. [[CrossRef](#)]
30. Anderson, D.J. Determination of the lower limit of detection. *Clin. Chem.* **1989**, *35*, 2152. [[CrossRef](#)]
31. Gans, P.; Sabatini, A.; Vacca, A. Investigation of equilibria in solution. Determination of equilibrium constants with the HYPERQUAD suite of programs. *Talanta* **1996**, *43*, 1739–1753. [[CrossRef](#)]
32. Beck, M.T.; Nagypál, I. *Chemistry of Complex Equilibria*; Ellis Horwood: Chichester, UK, 1990; 402p.
33. Schmittel, M.; Ammon, H. Synthesis and spectroscopy of new iron(II) complexes of 4,7-bis(aza-crown ether)-phenanthrolines with unusual complexation properties. *J. Chem. Soc. Chem. Commun.* **1995**, 687–688. [[CrossRef](#)]
34. Schmittel, M.; Lin, H.-W.; Thiel, E.; Meixner, A.J.; Ammon, H. Effects of multiple ion loading on redox and luminescence properties of ruthenium trisphenanthroline crown ether hybrids. *Dalton Trans.* **2006**, 4020–4028. [[CrossRef](#)]
35. Suzuki, H.; Kanbara, T.; Yamamoto, T. Ru(II) complexes with new redox-active 1,10-phenanthroline derivatives: Structural, spectral, and electrochemical investigations. *Inorg. Chim. Acta* **2004**, *357*, 4335–4340. [[CrossRef](#)]

36. Shan, G.-G.; Zhang, L.-Y.; Li, H.-B.; Wang, S.; Zhu, D.-X.; Li, P.; Wang, C.-G.; Su, Z.-M.; Liao, Y. A cationic iridium(III) complex showing aggregation-induced phosphorescent emission (AIPE) in the solid state: Synthesis, characterization and properties. *Dalton Trans.* **2012**, *41*, 523–530. [[CrossRef](#)]
37. Wu, K.; Zhang, T.; Zhan, L.; Zhong, C.; Gong, S.; Lu, Z.-H.; Yang, C. Tailoring optoelectronic properties of phenanthroline-based thermally activated delayed fluorescence emitters through isomer engineering. *Adv. Opt. Mater.* **2016**, *4*, 1558–1566. [[CrossRef](#)]
38. Louis, M.; Thomas, H.; Gmelch, M.; Haft, A.; Fries, F.; Reineke, S. Blue-light-absorbing thin films showing ultralong room-temperature phosphorescence. *Adv. Mater.* **2019**, *31*, 1807887. [[CrossRef](#)]
39. Liang, H.-P.; Acharjya, A.; Anito, D.A.; Vogl, S.; Wang, T.-X.; Thomas, A.; Han, B.-H. Rhenium-metalated polypyridine-based porous polycarbazoles for visible-light CO₂ photoreduction. *ACS Catal.* **2019**, *9*, 3959–3968. [[CrossRef](#)]
40. Wolfe, J.P.; Wagaw, S.; Marcoux, J.-F.; Buchwald, S.L. Rational development of practical catalysts for aromatic carbon–nitrogen bond formation. *Acc. Chem. Res.* **1998**, *31*, 805–818. [[CrossRef](#)]
41. Hartwig, J.F. Carbon–heteroatom bond-forming reductive eliminations of amines, ethers, and sulfides. *Acc. Chem. Res.* **1998**, *31*, 852–860. [[CrossRef](#)]
42. Ruiz-Castillo, P.; Buchwald, S.L. Applications of palladium-catalyzed C–N cross-coupling reactions. *Chem. Rev.* **2016**, *116*, 12564–12649. [[CrossRef](#)] [[PubMed](#)]
43. Beletskaya, I.P.; Cheprakov, A.V. Copper in cross-coupling reactions. *Coord. Chem. Rev.* **2004**, *248*, 2337–2364. [[CrossRef](#)]
44. Beletskaya, I.P.; Cheprakov, A.V. The complementary competitors: Palladium and copper in C–N cross-coupling reactions. *Organometallics* **2012**, *31*, 7753–7808. [[CrossRef](#)]
45. Wagaw, S.; Buchwald, S.L. The synthesis of aminopyridines: A method employing palladium-catalyzed carbon–nitrogen bond formation. *J. Org. Chem.* **1996**, *61*, 7240–7241. [[CrossRef](#)] [[PubMed](#)]
46. Shen, Q.; Shekhar, S.; Stambuli, J.P.; Hartwig, J.F. Highly Reactive, general, and long-lived catalysts for coupling heteroaryl and aryl chlorides with primary nitrogen nucleophiles. *Angew. Chem. Int. Ed.* **2005**, *44*, 1371–1375. [[CrossRef](#)]
47. Eggert, J.P.W.; Lüning, U.; Näther, C. Synthesis and functionalisation of 5-substituted neocuproine derivatives. *Eur. J. Org. Chem.* **2005**, *2005*, 1107–1112. [[CrossRef](#)]
48. Beletskaya, I.P.; Bessmertnykh, A.G.; Guillard, R. Palladium-catalyzed synthesis of aryl-substituted polyamine compounds from aryl halides. *Tetrahedron Lett.* **1997**, *38*, 2287–2290. [[CrossRef](#)]
49. Cook, T.R.; Stang, P.J. Recent developments in the preparation and chemistry of metallacycles and metallacages via coordination. *Chem. Rev.* **2015**, *115*, 7001–7045. [[CrossRef](#)]
50. Mede, T.; Jäger, M.; Schubert, U.S. “Chemistry-on-the-complex”: Functional Ru^{II} polypyridyl-type sensitizers as divergent building blocks. *Chem. Soc. Rev.* **2018**, *47*, 7577–7627. [[CrossRef](#)] [[PubMed](#)]
51. Balzani, V.; Juris, A.; Venturi, M.; Campagna, S.; Serroni, S. Luminescent and redox-active polynuclear transition metal complexes. *Chem. Rev.* **1996**, *96*, 759–834. [[CrossRef](#)] [[PubMed](#)]
52. Véry, T.; Ambrosek, D.; Otsuka, M.; Gourlaouen, C.; Assfeld, X.; Monari, A.; Daniel, C. Photophysical properties of ruthenium(II) polypyridyl DNA Intercalators: Effects of the molecular surroundings investigated by theory. *Chem. Eur. J.* **2014**, *20*, 12901–12909. [[CrossRef](#)] [[PubMed](#)]
53. Ghosh, A.; Ganguly, B.; Das, A. Urea-based ruthenium(II)–polypyridyl complex as an optical sensor for anions: Synthesis, characterization, and binding studies. *Inorg. Chem.* **2007**, *46*, 9912–9918. [[CrossRef](#)]
54. Juris, A.; Balzani, V.; Barigelletti, F.; Campagna, S.; Belser, P.; von Zelewsky, A. Ru(II) polypyridine complexes: Photophysics, photochemistry, electrochemistry, and chemiluminescence. *Coord. Chem. Rev.* **1988**, *84*, 85–277. [[CrossRef](#)]
55. Cook, M.J.; Lewis, A.P.; McAuliffe, G.S.G.; Skarda, V.; Thomson, A.J.; Gaspard, J.L.; Robbins, D.J. Luminescent metal complexes. Part 1. Tris-chelates of substituted 2,2′-bipyridyls with ruthenium (II) as dyes for luminescent solar collectors. *J. Chem. Soc. Perkin Trans.* **1984**, *2*, 1293–1301. [[CrossRef](#)]
56. Vos, J.G. Excited-state acid-base properties of inorganic compounds. *Polyhedron* **1992**, *11*, 2285–2299. [[CrossRef](#)]
57. Steinegger, A.; Wolfbeis, O.S.; Borisov, S.M. Optical sensing and imaging of pH values: Spectroscopies, materials, and applications. *Chem. Rev.* **2020**, *120*, 12357–12489. [[CrossRef](#)]
58. Chan, C.-M.; Wong, K.-Y. Evaluation of a luminescent ruthenium complex immobilized inside Nafion as optical pH sensor. *Analyst* **1998**, *123*, 1843–1847. [[CrossRef](#)]
59. Clarke, Y.; Xu, W.; Demas, J.N.; DeGraff, B.A. Lifetime-based pH sensor system based on a polymer-supported ruthenium(II) complex. *Anal. Chem.* **2000**, *72*, 3468–3475. [[CrossRef](#)]
60. Malins, C.; Glever, H.G.; Keyes, T.E.; Vos, J.G.; Dressick, W.J.; MacCraith, B.D. Sol–gel immobilised ruthenium(II) polypyridyl complexes as chemical transducers for optical pH sensing. *Sens. Actuators B* **2000**, *67*, 89–95. [[CrossRef](#)]
61. Hu, L.; Niu, C.; Zeng, G.; Wang, X.; Huang, D. Determination of dissolved oxygen in water based on its quenching effect on the fluorescent intensity of bis(2,2′-bipyridine)-5-amino-1,10-phenanthroline ruthenium complex. *Anal. Sci.* **2011**, *27*, 1121. [[CrossRef](#)]
62. Giordano, P.J.; Bock, C.R.; Wrighton, M.S. Excited state proton transfer of ruthenium(II) complexes of 4,7-dihydroxy-1,10-phenanthroline. Increased acidity in the excited state. *J. Am. Chem. Soc.* **1978**, *100*, 6960–6965. [[CrossRef](#)]
63. Thompson, A.M.W.C.; Smailes, M.C.C.; Jeffery, J.C.; Ward, M.D. Ruthenium tris-(bipyridyl) complexes with pendant protonatable and deprotonatable moieties: pH sensitivity of electronic spectral and luminescence properties. *J. Chem. Soc. Dalton Trans.* **1997**, 737–744. [[CrossRef](#)]

64. Granovsky, A.A. Firefly Version 8. Available online: <http://classic.chem.msu.su/gran/firefly/index.html> (accessed on 1 January 2022).
65. Schmidt, M.W.; Baldrige, K.K.; Boatz, J.A.; Elbert, S.T.; Gordon, M.S.; Jensen, J.H.; Koseki, S.; Matsunaga, N.; Nguyen, K.A.; Su, S.; et al. General atomic and molecular electronic structure system. *J. Comput. Chem.* **1993**, *14*, 1347–1363. [CrossRef]
66. Dolg, M.; Stoll, H.; Preuss, H.; Pitzer, R.M. Relativistic and correlation effects for element 105 (hahnium, Ha): A comparative study of M and MO (M = Nb, Ta, Ha) using energy-adjusted ab initio pseudopotentials. *J. Phys. Chem.* **1993**, *97*, 5852–5859. [CrossRef]
67. Bryantsev, V.S.; Diallo, M.S.; Goddard, W.A. pKa calculations of aliphatic amines, diamines, and aminoamides via density functional theory with a Poisson–Boltzmann continuum solvent model. *J. Phys. Chem. A* **2007**, *111*, 4422–4430. [CrossRef]
68. Abel, A.S.; Averin, A.D.; Cheprakov, A.V.; Roznyatovsky, V.A.; Denat, F.; Bessmertnykh-Lemeune, A.; Beletskaya, I.P. 6-Polyamino-substituted quinolines: Synthesis and multiple metal (Cu^{II}, Hg^{II} and Zn^{II}) monitoring in aqueous media. *Org. Biomol. Chem.* **2019**, *17*, 4243–4260. [CrossRef] [PubMed]
69. Ranyuk, E.; Uglov, A.; Meyer, M.; Bessmertnykh Lemeune, A.; Denat, F.; Averin, A.; Beletskaya, I.; Guilard, R. Rational design of aminoanthraquinones for colorimetric detection of heavy metal ions in aqueous solution. *Dalton Trans.* **2011**, *40*, 10491–10502. [CrossRef] [PubMed]
70. Ballardini, R.; Varani, G.; Indelli, M.T.; Scandola, F.; Balzani, V. Free energy correlation of rate constants for electron transfer quenching of excited transition metal complexes. *J. Am. Chem. Soc.* **1978**, *100*, 7219–7223. [CrossRef]
71. Ramdass, A.; Sathish, V.; Babu, E.; Velayudham, M.; Thanasekaran, P.; Rajagopal, S. Recent developments on optical and electrochemical sensing of copper(II) ion based on transition metal complexes. *Coord. Chem. Rev.* **2017**, *343*, 278–307. [CrossRef]
72. Sivaraman, G.; Iniya, M.; Anand, T.; Kotla, N.G.; Sunnapu, O.; Singaravadivel, S.; Gulyani, A.; Chellappa, D. Chemically diverse small molecule fluorescent chemosensors for copper ion. *Coord. Chem. Rev.* **2018**, *357*, 50–104. [CrossRef]
73. Okda, H.E.; El Sayed, S.; Ferreira, R.C.M.; Gonçalves, R.R.; Costa, S.P.G.; Raposo, M.M.M.; Martínez-Mañez, R.; Sancenón, F. *N,N*-Diphenylanilino-heterocyclic aldehyde-based chemosensors for UV-vis/NIR and fluorescence Cu(II) detection. *New J. Chem.* **2019**, *43*, 7393–7402. [CrossRef]
74. Okda, H.E.; El Sayed, S.; Otri, I.; Ferreira, R.C.M.; Costa, S.P.G.; Raposo, M.M.M.; Martínez-Mañez, R.; Sancenón, F. 2,4,5-Triaryl imidazole probes for the selective chromo-fluorogenic detection of Cu(II). Prospective use of the Cu(II) complexes for the optical recognition of biothiols. *Polyhedron* **2019**, *170*, 388–394. [CrossRef]
75. Tapiero, H.; Townsend, D.M.; Tew, K.D. Trace elements in human physiology and pathology. Copper. *Biomed. Pharmacother.* **2003**, *57*, 386–398. [CrossRef]
76. Bisaglia, M.; Bubacco, L. Copper ions and Parkinson's disease: Why is homeostasis so relevant? *Biomolecules* **2020**, *10*, 195. [CrossRef] [PubMed]
77. Rawle, S.C.; Moore, P.; Alcock, N.W. Synthesis and coordination chemistry of 1-(2',2''-bipyridyl-5'-yl-methyl)-1,4,8,11-tetraazacyclotetradecane L1. Quenching of fluorescence from [Ru(bipy)₂(L¹)]²⁺ by coordination of Ni^{II} or Cu^{II} in the cyclam cavity (bipy = 2,2'-bipyridine; cyclam = 1,4,8,11-tetraazacyclotetradecane). *J. Chem. Soc. Chem. Commun.* **1992**, 684–687. [CrossRef]
78. Bolletta, F.; Costa, I.; Fabbri, L.; Licchelli, M.; Montalti, M.; Pallavicini, P.; Prodi, L.; Zaccheroni, N. A [Ru^{II}(bipy)₃]-[1,9-diamino-3,7-diazanonane-4,6-dione] two-component system, as an efficient ON–OFF luminescent chemosensor for Ni²⁺ and Cu²⁺ in water, based on an ET (energy transfer) mechanism. *J. Chem. Soc. Dalton Trans.* **1999**, 1381–1386. [CrossRef]
79. Website of ERA. Available online: <https://www.epa.gov/eg/battery-manufacturing-effluent-guidelines-documents> (accessed on 1 January 2022).
80. Comba, P.; Krämer, R.; Mokhir, A.; Naing, K.; Schatz, E. Synthesis of new phenanthroline-based heteroditopic ligands—Highly efficient and selective fluorescence sensors for copper(II) ions. *Eur. J. Inorg. Chem.* **2006**, *2006*, 4442–4448. [CrossRef]
81. Lin, Q.-T.; Pei, L.-M.; Xu, W.-C.; Chao, H.; Ji, L.-N. [Ru(bpy)₂(pipdpa)]²⁺ as a highly sensitive and selective luminescent chemosensor for Cu²⁺ in aqueous solution. *Inorg. Chem. Commun.* **2012**, *16*, 104–106. [CrossRef]
82. Zhang, P.; Pei, L.; Chen, Y.; Xu, W.; Lin, Q.; Wang, J.; Wu, J.; Shen, Y.; Ji, L.; Chao, H. A Dinuclear ruthenium(II) complex as a one- and two-photon luminescent probe for biological Cu²⁺ detection. *Chem. Eur. J.* **2013**, *19*, 15494–15503. [CrossRef] [PubMed]
83. Cheng, F.; Tang, N.; Miao, K.; Wang, F. A dinuclear ruthenium(II) polypyridyl complex containing a terpy-like fragment for Cu²⁺ probing. *Z. Anorg. Allg. Chem.* **2014**, *640*, 1816–1821. [CrossRef]
84. Zheng, Z.-B.; Kang, S.-Y.; Zhao, Y.; Zhang, N.; Yi, X.; Wang, K.-Z. pH and copper ion luminescence on/off sensing by a dipyrzinylpyridine-appended ruthenium complex. *Sens. Actuators B* **2015**, *221*, 614–624. [CrossRef]
85. Liu, X.-W.; Xiao, Y.; Zhang, S.-B.; Lu, J.-L. A selective luminescent sensor for the detection of copper(II) ions based on a ruthenium complex containing DPA moiety. *Inorg. Chem. Commun.* **2017**, *84*, 56–58. [CrossRef]
86. Zheng, Z.-B.; Huang, Q.-Y.; Han, Y.-F.; Zuo, J.; Ma, Y.-N. Ruthenium(II) complex-based chemosensors for highly sensitive and selective sequential recognition of copper ion and cyanide. *Sens. Actuators B* **2017**, *253*, 203–212. [CrossRef]
87. Kumar, P.; Kumar, S. Copper ion luminescence on/off sensing by a quinoline-appended ruthenium(II)-polypyridyl complex in aqueous media. *J. Mol. Struct.* **2020**, *1202*, 127242. [CrossRef]
88. Meyer, M.; Frémond, L.; Espinosa, E.; Guilard, R.; Ou, Z.; Kadish, K.M. Synthesis, characterization, and X-ray crystal structures of cyclam derivatives. 5. Copper(II) binding studies of a pyridine-strapped 5,12-dioxocyclam-based macrobicycle. *Inorg. Chem.* **2004**, *43*, 5572–5587. [CrossRef] [PubMed]
89. Zhang, Y.; Liu, Z.; Zhang, Y.; Xu, Y.; Li, H.; Wang, C.; Lu, A.; Sun, S. A reversible and selective luminescent probe for Cu²⁺ detection based on a ruthenium(II) complex in aqueous solution. *Sens. Actuators B* **2015**, *211*, 449–455. [CrossRef]